PAPER

The stochastic field transport associated with the slab ITG modes

Plasma Phys. Control. Fusion **55** (2013) 125003 (13pp) doi:10.1088/0741-3335/55/12/125003

The stochastic field transport associated with the slab ITG modes

J W Connor[1,2,3], **R J Hastie**[1] **and A Zocco**[1,3]

[1] EURATOM/CCFE Fusion Association, Culham Science Centre, Abingdon, Oxon, OX14 3DB, UK
[2] Imperial College of Science, Technology and Medicine, London SW7 2BZ, UK
[3] Rudolf Peierls Centre for Theoretical Physics, 1 Keble Road, Oxford, OX1 3NP, UK

Received 20 June 2013, in final form 30 August 2013
Published 29 October 2013
Online at stacks.iop.org/PPCF/55/125003

Abstract
Many models for anomalous transport consider the turbulent $\boldsymbol{E} \times \boldsymbol{B}$ transport arising from electrostatic micro-instabilities. In this paper we investigate whether the perturbed magnetic field that is associated with such instabilities at small but finite values of β can lead to significant stochastic magnetic field transport. Using the tearing parity, long wavelength ion temperature gradient (ITG) modes in a plasma slab with magnetic shear as an example, we calculate the amplitude of the perturbed magnetic field at the resonant surface that results. The plasma model consists of a Braginskii description for the electrons with the dissipation at the resonant surface evaluated for the semi-collisional regime, while a finite ion Larmor radius kinetic model is invoked for the ions. The resulting stochastic field transport is estimated and also compared with an estimate for the $\boldsymbol{E} \times \boldsymbol{B}$ transport due to the ITG mode.

(Some figures may appear in colour only in the online journal)

1. Introduction

Calculations of anomalous transport due to micro-instabilities tend to concentrate on the contribution from the perturbed $\boldsymbol{E} \times \boldsymbol{B}$ drifts arising from electrostatic perturbations [1], although there are a number of studies of the cross-field transport arising from the stochastic magnetic fields associated with some electromagnetic instabilities, e.g. micro-tearing modes [2–6]. As one pushes closer to the β-limit ($\beta = 2\mu_0 nT/B^2$) in ITER the electromagnetic effects will become stronger and electron transport due to resulting stochastic magnetic fields may dominate. For a burning plasma where the electrons are heated by alpha-particles this is a matter for some concern. The growth rates of ITG modes actually decrease as one approaches the ideal MHD ballooning limit [7, 8], but there is some evidence that transport does not decrease [7, 9]. It is possible that the electromagnetic perturbation that inevitably accompanies a predominately electrostatic instability due to a small but finite value of β can produce significant stochastic field transport, perhaps exceeding the original $\boldsymbol{E} \times \boldsymbol{B}$ contribution or compensating for any decrease in $\boldsymbol{E} \times \boldsymbol{B}$ transport with β.

The purpose of the present paper is to investigate this possibility analytically using the long wavelength, slab-like, tearing parity ITG instabilities [10] as a simple example. The slab ITG branch only dominates the toroidal branch when $s/(2q) > 1$, with the shear, $s = (r/q)\mathrm{d}q/\mathrm{d}r$, q being the safety factor [11], or curvature effects are weak, $L_n/R \ll 1$, with L_n the density scale-length and R the tokamak major radius [12, 13], which are not typical situations in tokamak experiments. However the analysis for the slab case allows one to understand the subtle interplay of the very disparate spatial scales that characterize the ion and electron responses, in determining the perturbed magnetic field amplitude. It is a challenging task for numerical simulations to capture these widely different scales and this calculation will shed light on the extent to which this is necessary. Of course the corresponding ion response and subsequent analysis for the toroidal branch will be very different from that presented for the slab case in this paper.

The electrostatic ITG perturbation in slab geometry is dominated by long wavelengths, with $k_\perp \rho_\mathrm{i} \leqslant 1$ where $\rho_\mathrm{i} = (2m_\mathrm{i}T_\mathrm{i})^{1/2}/eB$ is the ion Larmor radius and $k_\perp$ is the wavenumber perpendicular to the magnetic field. However any magnetic field reconnection due to an associated electromagnetic component, as is required to produce a stochastic magnetic field, will occur at the much smaller scales where electron dissipative effects enter. Thus in modelling the ion dynamics we must consider a full Larmor radius (FLR) response for the ions in order to connect the long wavelength ITG perturbation to the reconnecting region of $k_\perp$. As an experimentally relevant model for the electrons we consider a semi-collisional description, when $\omega\nu_\mathrm{ei} \sim k_\parallel^2 v_\mathrm{the}^2$, where ω is the mode frequency, ν_e is the electron collision frequency,

$v_{\rm the}$ is the electron thermal speed, $v_{\rm the} = (2T_{\rm e}/m_{\rm e})^{1/2}$, and $k_\parallel = k_y x/L_{\rm s}$ is the wavelength along the magnetic field. Here $L_{\rm s} = Rq^2/(r\,{\rm d}q/{\rm d}r)$ is the magnetic shear-length and k_y is the wavenumber perpendicular to the magnetic field, $\boldsymbol{B}$, but within the equilibrium magnetic surface. Such semi-collisional effects are significant when electron collisional transport processes along the magnetic field compete with the mode frequency, allowing us to define a 'semi-collisional width', $\delta = {\rm e}^{-{\rm i}\pi/4}(\omega\nu_{\rm ei}/k_y^2(T_{\rm e}/m_{\rm e}))^{1/2}L_{\rm s}$.

To simplify the problem further we consider the 'flat-density' limit where the density scale-length, $L_n \to \infty$, order the wavelengths so that $b_0 = k_y^2\rho_{\rm i}^2/2 \sim (L_{T_{\rm i}}/L_{\rm s})^{1/2} \ll 1$ and normalize the frequencies such that $\omega = (\omega_{*T_{\rm i}}T_{\rm i}/m_{\rm i}L_{\rm s}^2)^{1/3}\bar{\omega}$. Here we have introduced the diamagnetic-like frequency $\omega_{*T_{\rm i}} = k_y T_{\rm i}/eBL_{T_{\rm i}}$ with $L_{T_{\rm i}}$ the scale-length of the ion temperature gradient. To develop a systematic ordering scheme, we consider $L_{T_{\rm i}}/L_{\rm s} \ll 1$, i.e. sharp ion temperature gradients, and introduce a parameter $\alpha = (b_0^2L_{\rm s}/L_{T_{\rm i}})^{2/3} \sim 0(1)$ so that $b_0 \sim (L_{T_{\rm i}}/L_{\rm s})^{1/2}$.

In standard tearing mode theory the amount of reconnection at a resonant surface depends in part on a quantity Δ' which represents the instability drive due to the current gradient. An equivalent quantity, Δ^*, encapsulating the effects of the tearing parity, long wavelength electrostatic ITG mode, appears in the present theory as a boundary condition at small values of k_x in Fourier space (although at larger values than those corresponding to the ITG mode itself, i.e. at $k_x\rho_{\rm i} \gg b_0^{1/2}$) and plays a part in determining the electromagnetic response in the vicinity of the resonant surface, where k_x is large. For the case of the semi-collisional electron model, this reconnecting region corresponds to a radial wavenumber given by $k_x \sim 1/\delta_0$, where we have introduced a real parameter, δ_0, to characterize the semi-collisional width [14, 15]. This is defined as $\delta_0 = |\delta(\omega)|$, evaluated at $\omega = (\omega_{*T_{\rm i}}T_{\rm i}/m_{\rm i}L_{\rm s}^2)^{1/3}$. Thus $\delta_0/\rho_{\rm i} = b_0^{-5/12}(m_{\rm e}/2m_{\rm i})^{1/4}(T_{\rm i}/T_{\rm e})^{1/2}(\nu_{\rm ei}L_{\rm s}/v_{\rm the})^{1/2}(L_{\rm s}/L_{T_{\rm i}})^{1/6}$. The calculation below aims to quantify the amount of reconnection and determine its implications for stochastic field transport.

This work complements two recent numerical simulations of stochastic magnetic transport arising from ITG turbulence, although from the toroidal rather than the slab branch. In [16] it was shown that magnetic stochasticity was always present at sufficiently short wavelengths for any value of β, but that the related transport was generally small. On the other hand, in [17] it was found that nonlinearly excited, subdominant, stable micro-tearing modes, rather than tearing parity ITG modes, were responsible for the stochastic magnetic field transport.

In section 2 we provide the fundamental equations describing the electromagnetic ITG modes and sketch the structure of the calculation. Section 3 determines the characteristics of the long wavelength electrostatic ITG modes while section 4 calculates the magnetic perturbations they drive in the same wavelength region. In order to connect this to the electromagnetic response in the electron layer, in section 5 we obtain the corresponding solution in the intermediate ion FLR region where $k_x\rho_{\rm i} \sim 0(1)$, matching it to the long wavelength solution using the quantity Δ^* introduced above. In section 6 we calculate the solution in the electron layer and, by matching it to the intermediate ion region solution in section 7, determine the magnetic perturbation at the resonant surface in section 8. In section 9 we estimate the resulting stochastic magnetic field transport and compare it with the electrostatic $E \times B$ transport associated with the original ITG mode. Conclusions are drawn in section 10.

2. Fundamental equations

In this section we establish the quasi-neutrality equation and Ampère's equation which determine the electromagnetic response to long wavelength, slab-like, electrostatic ITG modes and outline the sequence of steps in the subsequent calculation.

The equations describing the finite Larmor radius response of the ions to an electromagnetic perturbation in sheared slab geometry are derived in appendix A. Finite ion Larmor radius effects were discussed in [14, 15], but it is necessary to calculate the 'ion-sound' corrections in order to describe the slab ITG mode. Likewise the equations describing the electrons for semi-collisional plasma, i.e. when collisional transport processes along the magnetic field compete with the mode frequency, are derived in appendix B. Again such a model was also discussed in [14, 15], but it is now necessary to account for ion parallel motion in the Ohm's law. Substituting the calculated perturbed ion and electron densities into the quasi-neutrality equation provides one of the governing equations, while inserting the calculated perturbed current into Ampère's law provides the other.

To obtain the quasi-neutrality equation we use equation (A.10), which includes the 'ion-sound' corrections of $0(k_\parallel^2v_\parallel^2/\omega^2)$, for the perturbed ion density, $\delta n_{\rm i}$, while the perturbed electron density, $\delta n_{\rm e}$, is provided by the electron continuity equation, equation (B.1). However the latter equation involves the perturbed electron parallel velocity, $u_{\parallel{\rm e}}$, which is obtained in terms of the perturbed parallel component of the vector potential, $A_\parallel$, and the perturbed parallel ion velocity, $u_{\parallel{\rm i}}$, from equation (A.11) with the aid of Ampère's equation, equation (A.9). Similarly we use equation (B.6) for the perturbed parallel current, $j_\parallel$, again substituting for $u_{\parallel{\rm i}}$ from equation (A.11), to obtain Ampère's law for $A_\parallel$.

Introducing the flat-density ordering discussed in the Introduction, namely $b_0 = k_y^2\rho_{\rm i}^2/2 \sim (L_{T_{\rm i}}/L_{\rm s})^{1/2}$, with $L_{T_{\rm i}}/L_{\rm s} \ll 1$, and normalizing the frequencies such that $\omega = (\omega_{*T_{\rm i}}(T_{\rm i}/m_{\rm i}L_{\rm s}^2))^{1/3}\bar{\omega}$, simplifies the equations considerably. The quasi-neutrality equation takes the form:

$$\frac{i\tau\alpha^2}{\bar{\omega}^2\hat{\beta}_{\rm T}b_0^2}\frac{\rm d}{{\rm d}\bar{k}}(\bar{k}_\perp^2\hat{A}) = H\hat{\varphi} - \frac{b_0}{\bar{\omega}^3}\left[\frac{\rm d}{{\rm d}\bar{k}}\left(\frac{{\rm d}\hat{\alpha}_1}{{\rm d}\bar{k}}\hat{\varphi}\right) - {\rm i}\frac{{\rm d}\hat{\alpha}_1}{{\rm d}\bar{k}}\hat{A}\right]. \tag{1}$$

Ampère's law can be written

$$\frac{\tau^2\alpha^2}{\bar{\omega}^2\hat{\beta}_{\rm T}b_0^2}\frac{\delta^2}{\rho_{\rm i}^2}(\bar{k}_\perp^2\hat{A}) = \frac{(\hat{\sigma}_0 + d_1(x/\delta)^2)}{(1 + d_0(x/\delta)^2 + d_1(x/\delta)^4)}\left({\rm i}\frac{\rm d}{{\rm d}\bar{k}}\hat{\varphi} + \hat{A}\right) + \frac{2\tau b_0}{\bar{\omega}^3}\frac{x^2}{\rho_{\rm i}^2}\frac{(d_2 + d_1(x/\delta)^2)}{(1 + d_0(x/\delta)^2 + d_1(x/\delta)^4)} \times \left[\hat{\alpha}_1\left({\rm i}\frac{\rm d}{{\rm d}\bar{k}}\hat{\varphi} + \hat{A}\right) + \frac{\rm i}{2}\frac{{\rm d}\hat{\alpha}_1}{{\rm d}\bar{k}}\hat{\varphi}\right], \tag{2}$$

where we have introduced $\alpha = (b_0^2 L_s/L_{T_i})^{2/3} \sim 0(1)$ and $\bar{k} = k_x \rho_i$. In equation (2) we have used a mixed notation in x- and k_x-space, so that, if we consider these equations in k_x-space for example, we identify $x = -\mathrm{i}\mathrm{d}/\mathrm{d}k_x$ and *vice versa*. Other notation is as follows:

$$\hat{\varphi} = e\varphi/T_i, \quad \hat{A} = (\omega L_s/\bar{k}_y) e A_\parallel/T_i, \quad \hat{\beta}_T = \beta_e (L_s/L_{T_i})^2/2$$

with $\beta_e = 2\mu_0 n T_e/B^2$,

$$\tau = T_e/T_i, \quad H = \Gamma_0(b) - 1 + \frac{\alpha b}{b_0 \bar{\omega}}[\Gamma_0(b) - \Gamma_1(b)] - \frac{b_0}{\bar{\omega}^3 b}\left[(\bar{k}^2 - \bar{k}_y^2)\frac{\mathrm{d}\hat{\alpha}_1}{\mathrm{d}\bar{k}^2} + \bar{k}^2 \hat{\alpha}_2\right],$$

$$\hat{\alpha}_1 = \Gamma_0(b) - b(\Gamma_0 - \Gamma_1),$$

$$\hat{\alpha}_2 = [2(b-1)^2\Gamma_0(b) - b(2b-3)\Gamma_1(b)],$$

$$\hat{\sigma}_0 = 1.71 \frac{\tau\alpha}{\bar{\omega} b_0} \frac{L_{T_i}}{L_{T_e}}, \quad d_0 = 5.1,\ d_1 = 2.1,\ d_2 = 2.9,$$

$$b = \frac{\bar{k}_\perp^2}{2} = \frac{k_\perp^2 \rho_i^2}{2}, \quad \text{where } k_\perp^2 = k_y^2 + k_x^2$$

$$b_0 = \frac{k_y^2 \rho_i^2}{2}, \quad \delta = \exp(-\mathrm{i}\pi/4)\left(\frac{m_e \omega \nu_{ei}}{k_y^2 T_e}\right)^{1/2} L_s. \tag{3}$$

These equations can be used to determine the electromagnetic perturbations at the resonant surface driven by the long wavelength electrostatic ITG modes and estimate the associated stochastic field transport. The approach involves the following sequence of calculations based on an ordering of terms in $\hat{\beta}_T b_0^2 \ll 1$, but with $\hat{\beta}_T \sim 0(1)$:

- By including the ion-sound terms, determine the characteristics of the 'local', long wavelength (i.e. $k_x \sim k_y \sim b_0^{1/2}$), tearing parity, electrostatic ITG modes: φ_{ITG}.
- Calculate the associated, long wavelength, electromagnetic correction, $A_\parallel^{(1)}$, of $0(\hat{\beta}_T b_0^2)$, which introduces a constant of integration, c_0, corresponding to a vacuum solution of Ampère's equation.
- Calculate $\varphi^{(1)}$, the correction to φ_{ITG} driven by $A_\parallel^{(1)}$ in the long wavelength region. This provides a low k_x boundary condition for determining the 'non-local' $\varphi^{(1)}$ in the ion FLR region ($k_x \sim \rho_i^{-1} \gg k_y$).
- Calculate $\varphi^{(1)}$ for $k_x \sim \rho_i^{-1} \gg k_y$ using the above boundary condition (we also calculate the second order correction in $\hat{\beta}_T b_0^2$, $\varphi^{(2)}$, which helps to clarify the subsequent matching to the semi-collisional electron region).
- Determine the contributions to $A_\parallel$, driven by φ_{ITG}, $\varphi^{(1)}$ and $\varphi^{(2)}$ in the ion FLR region.
- Calculate $A_\parallel$ in the semi-collisional electron region ($k_x \sim \delta_0^{-1}$) satisfying the appropriate (i.e. even) boundary condition at $x = 0$.
- Determine the constant c_0 by matching electron and ion region solutions for $A_\parallel$; this matching also determines $A_\parallel(0)$, the amount of reconnection at the resonant surface, $x = 0$, in terms of φ_{ITG}.
- Calculate δB_x, the 'radial' perturbed magnetic field at the resonant surface, from $A_\parallel(0)$ and estimate the resulting stochastic field transport using the Rechester–Rosenbluth formula [18].

The above expansion involves a separation of electron and ion scales: $\delta_0 \ll \rho_i$. For consistency, this condition imposes a constraint, $1 \gg b_0 \gg (m_e/m_i)^{3/5}(\nu_{ei} L_s/v_{the})^{6/5}(L_s/L_{T_i})^{2/5}$, on our parameters; this is readily satisfied in hot tokamaks.

3. Slab ITG mode: $k_x \sim k_y$

Before discussing the slab ITG mode in detail it is helpful to consider equation (2) in the 'ion region', $x \sim \rho_i \gg \delta_0$ (i.e. $k_x \sim \rho_i^{-1} \ll \delta_0^{-1}$), where it simplifies considerably:

$$\frac{\tau^2\alpha^2}{\bar{\omega}^2 \hat{\beta}_T b_0^2} \frac{\mathrm{d}^2}{\mathrm{d}\bar{k}^2}(\bar{k}_\perp^2 \hat{A}) = -\left(\mathrm{i}\frac{\mathrm{d}}{\mathrm{d}\bar{k}}\hat{\varphi} + \hat{A}\right) + \frac{2\tau b_0}{\bar{\omega}^3}\frac{\mathrm{d}^2}{\mathrm{d}\bar{k}^2} \times \left[\hat{\alpha}_1\left(\mathrm{i}\frac{\mathrm{d}}{\mathrm{d}\bar{k}}\hat{\varphi} + \hat{A}\right) + \frac{\mathrm{i}}{2}\frac{\mathrm{d}\hat{\alpha}_1}{\mathrm{d}\bar{k}}\hat{\varphi}\right]. \tag{4}$$

To describe the electrostatic ITG mode we consider the limit $\hat{\beta}_T b_0^2 \ll 1$ so that we can ignore $\hat{A}$ on the right-hand side of equation (4). Taking the long wavelength limit ($b \ll 1$), when $\hat{\alpha} = 1 + 0(\bar{k}^2)$, we can integrate once to yield

$$\frac{\mathrm{i}\alpha\tau}{\bar{\omega}\hat{\beta}_T b_0}\frac{\mathrm{d}}{\mathrm{d}\bar{k}}(\bar{k}_\perp^2 \hat{A}) = \frac{\bar{\omega} b_0}{\alpha\tau}\left(1 - \frac{2\tau b_0}{\bar{\omega}^3}\frac{\mathrm{d}^2}{\mathrm{d}\bar{k}^2}\right)\hat{\varphi}. \tag{5}$$

Substituting for $\hat{A}$ from equation (1), where $H \simeq \alpha b/\bar{\omega} b_0$ and $\hat{\alpha}_1 \simeq 1$ in the same limit, so that we can ignore the second term on the right-hand side, we obtain the equation for the long wavelength, electrostatic ITG modes:

$$L^{(0)}\hat{\varphi}^{(0)} \equiv \frac{2\tau b_0}{\bar{\omega}^3}\frac{\mathrm{d}^2}{\mathrm{d}\bar{k}^2}\hat{\varphi}^{(0)} + \left(\frac{\alpha\tau}{2 b_0 \bar{\omega}}\bar{k}_\perp^2 - 1\right)\hat{\varphi}^{(0)} = 0. \tag{6}$$

Since we are interested in electromagnetic effects with finite $A_\parallel$ at the resonant surface we consider the tearing parity solutions, i.e. those odd in $\bar{k}$:

$$\hat{\varphi}_n^{(0)} \equiv \hat{\varphi}_{ITG} = c_n H_{2n+1}((\lambda_n/b_0)^{1/2}\bar{k})\exp(-\lambda_n \bar{k}^2/2b_0)\varphi_0. \tag{7}$$

Here the index n labels the various harmonic solutions of equation (6) with eigenvalues $\bar{\omega} = \bar{\omega}_n$, $c_n = (2^{2n+1}\sqrt{\pi}\Gamma(2n+2))^{-1/2}$ is a normalization constant, H_{2n+1} is the Hermite polynomial and $\lambda_n = -\mathrm{i}\alpha^{1/2}\bar{\omega}_n/2$, so that $\mathrm{Re}\,\lambda_n > 0$ when $\mathrm{Im}\,\bar{\omega}_n > 0$. We have labelled the amplitude of the ITG mode by φ_0 and intend, ultimately, to relate the amplitude of the perturbed magnetic field to it.

The condition on the eigenvalue, $\bar{\omega}_n$, is

$$\bar{\omega}_n^2 - \alpha\tau\bar{\omega}_n - (2n+1)\mathrm{i}\alpha^{1/2}\tau = 0. \tag{8}$$

The solution for $\bar{\omega}_n$ depends on the parameter α. It will be interesting later to consider two limiting cases:

$$\text{(i) } \alpha \ll [4(2n+1)/\tau]^{2/3}, \tag{9}$$

when $\bar{\omega}_n = [(2n+1)\tau]^{1/2}\alpha^{1/4}\mathrm{e}^{\mathrm{i}\pi/4}$ and $\lambda_n = [(2n+1)\tau]^{1/2}\alpha^{3/4}\mathrm{e}^{-\mathrm{i}\pi/4}/2$;

$$\text{(ii) } \alpha \gg [4(2n+1)/\tau]^{2/3}, \tag{10}$$

when $\bar{\omega}_n = \tau\alpha + (2n+1)\mathrm{i}/\alpha^{1/2}$ and $\lambda_n = [-\mathrm{i}\tau\alpha^{3/2} + (2n+1)]/2$. Clearly for higher values of n the result (i)

prevails for all α. Furthermore, the higher n harmonics, which correspond to higher radial harmonics in x-space, have larger growth rates and radial wavenumbers. Thus forming the expectation value of $\bar{k}^2$ over the eigen-function (7), we obtain $\langle \bar{k}^2 \rangle_n = (n+1/2)b_0/\lambda_n \sim (n+1/2)^{1/2} b_0$. Of course the maximum acceptable value of n is limited by the two approximations: (a) $\delta_0/\rho_i \ll 1$, where $\delta_0 \propto \bar{\omega}_n^{1/2} \propto n^{1/4}$; (b) $\langle \bar{k}^2 \rangle_{\rm ITG} \ll 1$, with $\langle \bar{k}^2 \rangle_{\rm ITG} \sim n b_0/\lambda_n \propto n^{1/2}$.

4. Electromagnetic corrections for $k_x \sim k_y$

This section provides a calculation of the long wavelength, electromagnetic perturbations driven by the ITG modes. Thus, in next order in $\hat{\beta}_T b_0^2$ we obtain $\hat{A}^{(1)}$ by integrating equation (1):

$$\bar{k}_\perp^2 \hat{A}^{(1)} = c_0 - i\frac{\bar{\omega}_n \hat{\beta}_T b_0}{2\tau\alpha} \int_0^{\bar{k}} d\bar{k}\, \bar{k}_\perp^2 \hat{\varphi}_{\rm ITG}, \tag{11}$$

with c_0 a constant of integration of order $\hat{\beta}_T b_0^2$. In turn $\hat{A}^{(1)}$ drives a correction to $\hat{\varphi}_{\rm ITG}$, $\hat{\varphi}^{(1)}$, which is non-local in $\bar{k}$, i.e. not restricted to $k_x \sim k_y$. However, we first determine $\hat{\varphi}^{(1)}$ for $k_x \sim k_y$ to provide the boundary condition for $\hat{\varphi}^{(1)}$ in the region $\bar{k} \sim 1$, which we calculate in the next section.

Integrating equation (4) once in $\bar{k}$ and substituting for $\bar{k}_\perp^2 \hat{A}^{(1)}$ from equation (5), we have

$$L^{(0)}\hat{\varphi}^{(1)} = c_1 - i\int_0^{\bar{k}} d\bar{k}\, \hat{A}^{(1)} + i\frac{2\tau b_0}{\bar{\omega}_n^3}\frac{d}{d\bar{k}}\hat{A}^{(1)} - \delta\bar{\omega}_n \left.\frac{\partial L^{(0)}}{\partial \bar{\omega}}\right|_{\bar{\omega}_n} \hat{\varphi}_{\rm ITG} \equiv R(\bar{k}), \tag{12}$$

where c_1 is a second constant of integration and $\delta\bar{\omega}_n$ is a correction to $\bar{\omega}_n$. Since we seek a tearing parity solution $\hat{\varphi}^{(1)}$ (i.e. odd in $\bar{k}$), we take $c_1 = 0$. On the other hand, the constant c_0 in equation (11) emerges, ultimately, as the 'eigenvalue' of the present calculation: i.e. it will eventually be determined by matching solutions through an intermediate region where $\bar{k} \sim 0(1)$, to an electron region (a layer around $x = 0$ in configuration space, corresponding to the region $\bar{k} \geqslant \rho_i/\delta_0$ in transform space) and application of appropriate boundary conditions as $\bar{k} \to \infty$. Along with the final determination of c_0 the complete structure of the electromagnetic eigenmode, i.e. both $\hat{A}(\bar{k})$ and $\hat{\varphi}(\bar{k})$, will then be specified. In particular the amplitude of the magnetic perturbation at the resonant surface, $\delta B_x/B$ at $x = 0$, relative to that of the underlying 'electrostatic' ITG mode, which remains arbitrary within this linear theory.

Annihilating $\hat{\varphi}^{(1)}$ in equation (12) by applying the operation, $\int_0^\infty d\bar{k}\hat{\varphi}_{\rm ITG}(\bar{k})...$ we obtain the condition

$$\int_0^\infty d\bar{k}\hat{\varphi}_{\rm ITG}(\bar{k})R(\bar{k}) = 0, \tag{13}$$

which provides an equation for $\delta\bar{\omega}_n$, although this is not needed for our present purposes.

A solution for $\hat{\varphi}^{(1)}$ in terms of $R(\bar{k})$ from equation (12) satisfying the appropriate boundary conditions can be obtained by the method of variation of parameters using the two solutions of the homogeneous equation (6). These are the parabolic cylinder functions: $U(-(n+1/2), z)$ and $V(-(n+1/2), z)$ where $z = (2\lambda/b_0)^{1/2}\bar{k}$ [19]. (Note solution (7) is essentially the exponentially decaying function $U(-(n+1/2), z)$ and condition (13) ensures there is no exponential growth from the $V(-(n+1/2), z)$ contribution.)

However, we can determine the required features of the solution without formally constructing this expression. Thus at small k we require $\hat{\varphi}^{(1)}$ to satisfy the ideal MHD condition, $E_\parallel = 0$. It is evident from equation (12) that the dominant terms when $\bar{k}^2 \ll b_0$ originate from the 'ion-sound' terms [20, 21] and are

$$\frac{\tau b_0}{\bar{\omega}_0^3}\frac{d}{d\bar{k}}\left(i\frac{d}{d\bar{k}}\hat{\varphi}^{(1)} + \hat{A}^{(1)}\right) \propto \frac{d}{d\bar{k}}\hat{E}_\parallel. \tag{14}$$

Clearly in x-space this implies $xE_\parallel \simeq 0$, i.e. $E_\parallel \simeq 0$ at large x. In $\bar{k}$-space, integration of equation (14) introduces an arbitrary constant but this becomes a δ-function in x-space and is therefore irrelevant to the large x region. The small $\bar{k}$ form of the solution in terms of parabolic cylinder functions discussed above confirms this result.

The information we actually need from $\hat{\varphi}^{(1)}$ is its behaviour when $1 > \bar{k} > b_0^{1/2}$ in order to provide a low $\bar{k}$ boundary condition for the solution in the $\bar{k} \sim 1$ region. This is readily obtained from equation (12), recalling the definition of the operator L in equation (6), to yield:

$$\hat{\varphi}^{(1)} \simeq \frac{2b_0\bar{\omega}_n}{\alpha\tau}\frac{R(\bar{k})}{\bar{k}^2}, \tag{15}$$

a result again confirmed from the large z asymptotic form of the solution in terms of parabolic cylinder functions. The decrease in $\hat{\varphi}^{(1)}$ with radial wavenumber k_x, evident in equation (15), is physically the result of finite ion Larmor radius averaging of the perturbation. It remains to determine the form of $R(\bar{k})$ in this region of $\bar{k}$. Clearly from its definition in equation (12), $R(\bar{k})$ is dominated by the contribution from the integral term $\int_0^{\bar{k}} d\bar{k}\, \hat{A}^{(1)}$, where $\hat{A}^{(1)}$ is given by equation (11), since the term in $\delta\bar{\omega}_n$ involves the localized solution $\hat{\varphi}_{\rm ITG}$ obtained in equation (7) and the contribution from $d\hat{A}^{(1)}/d\bar{k}$ is smaller by a factor $b_0/\bar{k}^2$. Evaluating this dominant term we obtain

$$R(\bar{k}) = -i\frac{c_0}{\bar{k}_y}\tan^{-1}\left(\frac{\bar{k}}{\bar{k}_y}\right) - \frac{\bar{\omega}_n\hat{\beta}_T b_0\varphi_0}{2\alpha\tau}\int_0^{\bar{k}}\frac{d\bar{k}}{\bar{k}_\perp^2} \times \int_0^{\bar{k}} d\bar{k}' c_n H_{2n+1}\left(\left(\frac{\lambda_n}{b_0}\right)^{1/2}\bar{k}'\right)\bar{k}'^2_\perp \exp\left(-\frac{\lambda_n\bar{k}'^2}{2b_0}\right). \tag{16}$$

Integrating by parts yields:

$$R(\bar{k}) = -i\frac{c_0}{\bar{k}_y}\tan^{-1}\left(\frac{\bar{k}}{\bar{k}_y}\right) - \frac{\bar{\omega}_n\hat{\beta}_T b_0^2\varphi_0}{2\alpha\tau}c_n\left(\frac{2}{\lambda_n}\right)^{1/2} \times \int_0^{y(\bar{k})} dy' \left[\tan^{-1}\left(\frac{y(\bar{k})}{\sqrt{2\lambda_n}}\right) - \tan^{-1}\left(\frac{y'}{\sqrt{2\lambda_n}}\right)\right] \times \left(1 + \frac{y'^2}{2\lambda_n}\right)\exp\left(-\frac{y'^2}{2}\right)H_{2n+1}(y'), \tag{17}$$

where $y = \exp(-\mathrm{i}\pi/4)(\bar{\omega}_n\alpha^{1/2}/2b_0)^{1/2}\bar{k}$. Evaluating expression (17) in the limit $1 \gg \bar{k} \gg \bar{k}_y = (2b_0)^{1/2}$ we obtain

$$\begin{aligned} R(\bar{k}) &\sim R_0 + \frac{R_1}{\bar{k}} \\ &\equiv -\mathrm{i}\frac{\pi}{2}\frac{1}{\sqrt{2b_0}}\left\{c_0 - \mathrm{i}\frac{\bar{\omega}_n\hat{\beta}_{\mathrm{T}}b_0^{5/2}}{\alpha\tau}F_n(\lambda_n)\varphi_0\right\} \\ &\quad + \mathrm{i}\left\{c_0 - \mathrm{i}\frac{\bar{\omega}_n\hat{\beta}_{\mathrm{T}}b_0^{5/2}}{\alpha\tau}G_n(\lambda_n)\varphi_0\right\}\frac{1}{\bar{k}}, \end{aligned} \tag{18}$$

where

$$\begin{aligned} F_n(\lambda_n) &= \frac{c_n}{\sqrt{\lambda_n}}\int_0^\infty \mathrm{d}y'\left[1 - \frac{2}{\pi}\tan^{-1}\left(\frac{y'}{\sqrt{2\lambda_n}}\right)\right]\left(1 + \frac{y'^2}{2\lambda_n}\right) \\ &\quad \times \exp\left(-\frac{y'^2}{2}\right)H_{2n+1}(y'), \\ G_n(\lambda_n) &= \frac{c_n}{\sqrt{\lambda_n}}\int_0^\infty \mathrm{d}y'\left(1 + \frac{y'^2}{2\lambda_n}\right)\exp\left(-\frac{y'^2}{2}\right)H_{2n+1}(y'). \end{aligned} \tag{19}$$

Although the function $R(\bar{k})$ has some structure with peaks around $\bar{k} \sim 1$, its asymptotic form, represented by the quantities R_0 and R_1 and which sets in for $\bar{k} \geqslant 2$, encapsulates all the information concerning the long wavelength electrostatic ITG modes that we require.

5. The ion FLR region: $\bar{k} \sim 1$

The purpose of this section is to determine the electromagnetic perturbation driven by the long wavelength ITG mode in the region of k_x-space where finite ion Larmor radius effects are important, which can in turn be matched to the short wavelength response in the electron layer.

But first, as an aside, we note that in conventional tearing mode theory [22] one matches the perturbed electrostatic potential $\hat{\varphi}$ to an external ideal MHD form at low $\bar{k}$:

$$\hat{\varphi} \sim 1 + \frac{\Delta'\rho_{\mathrm{i}}}{\pi\bar{k}}, \tag{20}$$

where we recall that in ideal MHD $\rho_{\mathrm{i}}\Delta' = -2\bar{k}_y \equiv -2\sqrt{2b_0}$ for high wavenumbers of stable tearing modes. Now, however, because of the ion dynamics it is the solution (15) that provides the boundary condition at low $\bar{k}$ for determining the non-local $\varphi^{(1)}$, which we now calculate. Thus, we must match to the form

$$\hat{\varphi} \sim \frac{1}{\bar{k}^2}\left(1 + \frac{\Delta^*}{\bar{k}}\right), \tag{21}$$

where

$$\Delta^* = \frac{R_1}{R_0} = -\frac{2\sqrt{2b_0}}{\pi}\frac{\left\{c_0 - \dfrac{\mathrm{i}\bar{\omega}_n\hat{\beta}_{\mathrm{T}}b_0^{5/2}}{\alpha\tau}G_n(\lambda_n)\varphi_0\right\}}{\left\{c_0 - \dfrac{\mathrm{i}\bar{\omega}_n\hat{\beta}_{\mathrm{T}}b_0^{5/2}}{\alpha\tau}F_n(\lambda_n)\varphi_0\right\}}. \tag{22}$$

We return to the calculation of $\hat{\varphi}^{(1)}$ in the ion FLR region where $\bar{k} \sim 1 \gg \bar{k}_y \sim \sqrt{2b_0}$ and the ion-sound effects (i.e. terms involving $b_0\mathrm{d}^2/\mathrm{d}\bar{k}^2$) are negligible. Equations (1) and (4) then simplify considerably to yield an equation for $\hat{\varphi}^{(1)}$:

$$\frac{\mathrm{d}}{\mathrm{d}\bar{k}}\bar{k}_\perp^2\frac{\mathrm{d}}{\mathrm{d}\bar{k}}[(\tau H_0(\bar{k}_\perp) - 1)\hat{\varphi}^{(1)}] = 0, \tag{23}$$

where

$$H_0 = \Gamma_0 - 1 + \frac{\alpha\bar{k}_\perp^2}{2b_0\bar{\omega}_n}(\Gamma_0 - \Gamma_1). \tag{24}$$

This has the solution

$$(\tau H_0(\bar{k}_\perp) - 1)\hat{\varphi}^{(1)} = \frac{c_0'}{\bar{k}_y}\tan^{-1}\left(\frac{\bar{k}}{\bar{k}_y}\right) + c_1', \tag{25}$$

so that, for $\bar{k}_y \ll \bar{k} \ll 1$,

$$\hat{\varphi}^{(1)} \sim \frac{2b_0\bar{\omega}_n}{\alpha\tau}\left[\frac{c_0'}{\bar{k}_y}\left(\frac{\pi}{2} - \frac{\bar{k}_y}{\bar{k}}\right) + c_1'\right]\frac{1}{\bar{k}^2}. \tag{26}$$

Matching to solution (15) and recalling the form (18) for $R(\bar{k})$ when $\bar{k} \ll 1$, we obtain equations that determine c_0' and c_1':

$$\frac{\pi}{2}\frac{c_0'}{\bar{k}_y} + c_1' = R_0, \qquad c_0' = -R_1. \tag{27}$$

In the region $\bar{k} \gg 1$, where $H_0(\bar{k}) \sim -1 + \Lambda/\bar{k}$ with $\Lambda = (1+\alpha/2b_0\bar{\omega}_n)/\sqrt{\pi}$, the solution (25) takes the asymptotic form

$$\hat{\varphi}^{(1)} = -\frac{1}{(1+\tau)}\left(R_0 + \left(R_1 + \frac{\Lambda R_0\tau}{(1+\tau)}\right)\frac{1}{\bar{k}}\right), \tag{28}$$

on making the substitutions (27). To next order in $\hat{\beta}_{\mathrm{T}}b_0^2$, equation (23) becomes

$$\frac{\mathrm{d}}{\mathrm{d}\bar{k}}\bar{k}_\perp^2\frac{\mathrm{d}}{\mathrm{d}\bar{k}}[(\tau H_0(\bar{k}_\perp) - 1)\hat{\varphi}^{(2)}] + \frac{\bar{\omega}_n^2\hat{\beta}_{\mathrm{T}}b_0^2}{\tau\alpha^2}H_0(\bar{k}_\perp)\hat{\varphi}^{(1)} = 0 \tag{29}$$

and we find the correction $\varphi^{(2)}$, which in the limit $\bar{k} \gg 1$ takes the form

$$\hat{\varphi}^{(2)} = \frac{\bar{\omega}_n^2\hat{\beta}_{\mathrm{T}}b_0^2}{\alpha^2\tau(1+\tau)^2}\left(R_0\ln\bar{k} + \frac{(\Lambda R_0 - R_1)}{\bar{k}}\ln\bar{k} + 0\left(\frac{1}{\bar{k}}\right)\right). \tag{30}$$

Introducing the local ITG contribution $\hat{\varphi}_{\mathrm{ITG}}$ and the non-local contributions $\hat{\varphi}^{(1)}$ and $\hat{\varphi}^{(2)}$ into equation (1) provides an equation for $\hat{A}(\bar{k})$ (retaining terms up to two orders in $\hat{\beta}_{\mathrm{T}}b_0^2$) in the region $\bar{k} \gg 1$:

$$\bar{k}_\perp^2\hat{A} = c_0 - \mathrm{i}\frac{\bar{\omega}_n^2\hat{\beta}_{\mathrm{T}}b_0^2}{\tau\alpha^2}\int_0^{\bar{k}}\mathrm{d}\bar{k}H_0(\bar{k})(\hat{\varphi}_{\mathrm{ITG}} + \hat{\varphi}^{(1)} + \hat{\varphi}^{(2)}). \tag{31}$$

At large $\bar{k}$ the integration over the ITG contribution, $\hat{\varphi}_{\mathrm{ITG}}$, yields a constant, while for the non-local contributions, $\hat{\varphi}^{(1)}$ and $\hat{\varphi}^{(2)}$, one inserts the results (28) and (30) and uses the asymptotic form of $H_0(\bar{k})$ to obtain

$$\begin{aligned} \hat{A}(\bar{k}) &\sim -\mathrm{i}\frac{R_1}{\bar{k}^2}\left(1 + \frac{\bar{\omega}_n^2\hat{\beta}_{\mathrm{T}}b_0^2}{\alpha^2\tau(1+\tau)}\ln\bar{k}\right) - \mathrm{i}\frac{\bar{\omega}_n^2\hat{\beta}_{\mathrm{T}}b_0^2}{\alpha^2\tau(1+\tau)}\frac{R_0}{\bar{k}} \\ &\quad \times\left(1 - \frac{\bar{\omega}_n^2\hat{\beta}_{\mathrm{T}}b_0^2}{\alpha^2\tau(1+\tau)}\ln\bar{k} - \frac{\Lambda}{(1+\tau)}\frac{\ln\bar{k}}{\bar{k}}\right), \end{aligned} \tag{32}$$

where we have retained logarithmic corrections in order to match fully to the electron region solution. (The integral over $\bar{k}$ of $\hat{\varphi}^{(1)}$ also produces a term proportional to $\bar{k}^{-2}$, but this is smaller by order $\hat{\beta}_{\mathrm{T}}b_0^2$ than the term retained in equation (32).)

We shall see that the same term involving Λ is present in the electron region solution and so matches automatically. It is then helpful to recognize that equation (32) is the low $\hat{\beta}_{\mathrm{T}}b_0^2$ expansion of an expression involving two power laws:

$$\hat{A}(\bar{k}) \sim -\mathrm{i}R_1\bar{k}^{-(\nu_+ +1)} - \mathrm{i}\frac{\bar{\omega}_n^2\hat{\beta}_{\mathrm{T}}b_0^2}{\alpha^2\tau(1+\tau)}R_0\bar{k}^{-(\nu_- +1)}, \tag{33}$$

where

$$\nu_\pm = \frac{1}{2} \pm \left(\frac{1}{4} - \frac{\bar{\omega}_n^2\hat{\beta}_{\mathrm{T}}b_0^2}{\tau(1+\tau)\alpha^2}\right)^{1/2}. \tag{34}$$

We see that the quantity $\Delta^* = R_1/R_0$ in equation (33) continues to play a key role in the matching condition.

6. The electron layer: $\bar{k} \sim \rho_{\mathrm{i}}/\delta_0$

To investigate the extent of anomalous transport due to the magnetic field perturbation associated with the electrostatic ITG mode we must relate the magnitude of the magnetic perturbation at the resonant surface, $x = 0$, to the amplitude of the ITG mode. This involves solving for the perturbed magnetic potential in the electron region of k_x-space, $\bar{k} \sim \rho_{\mathrm{i}}/\delta_0$, and then matching the resulting expression in the limit $\bar{k}\delta_0/\rho_{\mathrm{i}} \ll 1$ to the form (33) from the ion region. In this section we obtain the electron region solution satisfying the correct boundary condition at $x = 0$.

In the limit $\bar{k} \gg 1$ we can solve equation (1) for $\hat{\varphi}(\bar{k})$ in terms of $\hat{A}(\bar{k})$:

$$\hat{\varphi} = -\frac{\mathrm{i}\tau\alpha^2}{\bar{\omega}_n^2\hat{\beta}_{\mathrm{T}}b_0^2}\left(1 - \frac{\Lambda}{\bar{k}}\right)\frac{\mathrm{d}}{\mathrm{d}\bar{k}}(\bar{k}_\perp^2\hat{A}), \tag{35}$$

where we have introduced the large $\bar{k}$ expansion of $H_0(\bar{k})$. After simplifying equation (2) in the limit $x \sim \delta_0 \ll \rho_{\mathrm{i}}$, and substituting for $\hat{\varphi}(\bar{k})$ from equation (35), ignoring the correction from the term $\Lambda/\bar{k}$, we obtain an equation for $\hat{A}$ in x-space:

$$\frac{\tau^2\alpha^2}{\bar{\omega}_n^2\hat{\beta}_{\mathrm{T}}b_0^2}\frac{\mathrm{d}^2}{\mathrm{d}s^2}\hat{A} = -\frac{(\hat{\sigma}_0 + \mathrm{d}_1 s^2)}{(1 + \mathrm{d}_0 s^2 + \mathrm{d}_1 s^4)}\left(\hat{A} + \frac{\tau\alpha^2 s^2}{\bar{\omega}_n^2\hat{\beta}_{\mathrm{T}}b_0^2}\frac{\mathrm{d}^2}{\mathrm{d}s^2}\hat{A}\right), \tag{36}$$

where we have introduced $s = x/\delta$, i.e. we have scaled x to the complex electron semi-collisional width. Equation (36) can be re-arranged to yield

$$\frac{\mathrm{d}^2}{\mathrm{d}s^2}\hat{A} = -\frac{\bar{\omega}_n^2\hat{\beta}_{\mathrm{T}}b_0^2}{\tau^2\alpha^2}\hat{\sigma}(s^2)\hat{A}, \tag{37}$$

where

$$\hat{\sigma}(s^2) = \frac{\hat{\sigma}_0 + d_1 s^2}{1 + (d_0 + \hat{\sigma}_0/\tau)s^2 + d_1(1+\tau)s^4/\tau}. \tag{38}$$

Invoking the low $\hat{\beta}_{\mathrm{T}}b_0^2$ expansion we can iterate the solution of equation (36):

$$\hat{A} = A_0\left[1 - \frac{\bar{\omega}_n^2\hat{\beta}_{\mathrm{T}}b_0^2}{\tau^2\alpha^2}\int_0^s \mathrm{d}s'\int_0^{s'}\mathrm{d}s''\hat{\sigma}(s''^2)\right]. \tag{39}$$

Recalling that our eventual aim is to calculate $A(0)$, the value of A at the resonant surface, $s = 0$, we need to determine the coefficient A_0 in equation (39).

The repeated integral in equation (39) can be evaluated straightforwardly and the limit $s \to \infty$ taken. On exploiting the condition $\hat{\sigma}_0 \gg 1$, this leads to

$$\hat{A} = A_0\left\{1 - \frac{\bar{\omega}_n^2\hat{\beta}_{\mathrm{T}}b_0^2}{\tau^2\alpha^2}\left[\frac{\pi\sqrt{\tau\hat{\sigma}_0}}{2}s - \frac{\tau}{1+\tau}\ln s\right]\right\}, \quad s \to \infty. \tag{40}$$

We must relate this solution to its transform in $\bar{k}$-space to link the amplitude A_0 to the quantity c_0 introduced in equation (11). In order to do this, it is convenient to consider the asymptotic form of the solution of equation (37) for finite values of $\hat{\beta}_{\mathrm{T}}b_0^2$:

$$\hat{A} = b_+ s^{\nu_+} + b_- s^{\nu_-}; \qquad \nu_\pm = \frac{1}{2} \pm \left(\frac{1}{4} - \frac{\bar{\omega}_n^2\hat{\beta}_{\mathrm{T}}b_0^2}{\tau(1+\tau)\alpha^2}\right)^{1/2}. \tag{41}$$

Now taking the limit $\hat{\beta}_{\mathrm{T}}b_0^2 \ll 1$ we have

$$\hat{A} \to b_+ s + b_-\left(1 + \frac{\bar{\omega}_n^2\hat{\beta}_{\mathrm{T}}b_0^2}{\tau(1+\tau)\alpha^2}\ln s\right), \tag{42}$$

so that we can identify b_+ and b_- by comparing expressions (40) and (42). Thus

$$b_+ = -\frac{\pi}{2}\frac{\sqrt{1.71}\hat{\beta}_{\mathrm{T}}}{\tau}\left(\frac{L_{T_{\mathrm{i}}}}{L_{T_{\mathrm{e}}}}\right)^{1/2}\left(\frac{\bar{\omega}_n b_0}{\alpha}\right)^{3/2}A_0 \tag{43}$$

(where we have substituted for $\hat{\sigma}_0$ from its definition in equation (3)), so that A_0 is determined by the value of b_+. Furthermore,

$$\frac{b_+}{b_-} = -\frac{\pi}{2}\frac{\sqrt{1.71}\hat{\beta}_{\mathrm{T}}}{\tau}\left(\frac{L_{T_{\mathrm{i}}}}{L_{T_{\mathrm{e}}}}\right)^{1/2}\left(\frac{\bar{\omega}_n b_0}{\alpha}\right)^{3/2}. \tag{44}$$

The form (41) can be used to calculate the transform of $\hat{A}$ in $\bar{k}$-space (recalling $\hat{A}(s)$ is an even function of s [15]):

$$\hat{A}(t) = b_+ t^{-(\nu_+ +1)}\cos\left[(\nu_+ +1)\frac{\pi}{2}\right]\Gamma(\nu_+ +1) + b_- t^{-(\nu_- +1)} \times \cos\left[(\nu_- +1)\frac{\pi}{2}\right]\Gamma(\nu_- +1), \tag{45}$$

where $t = (\delta/\rho_{\mathrm{i}})\bar{k}$. Taking the limit $\hat{\beta}_{\mathrm{T}}b_0^2 \ll 1$, we obtain

$$\hat{A}(t) \simeq -b_+ t^{-(\nu_+ +1)} - \frac{\pi}{2}\frac{\bar{\omega}_n^2\hat{\beta}_{\mathrm{T}}b_0^2}{\alpha^2\tau(1+\tau)}b_- t^{-(\nu_- +1)}. \tag{46}$$

We can iterate on this solution to calculate the correction arising from the $\Lambda/\bar{k}$ term in equation (35) and find it is identical to the related term in the ion region equation (32). The form of the solution (46) thus has an identical structure to that in equation (33) and the two can therefore be matched asymptotically.

7. Matching electron and ion region solutions

In this section we first obtain the constant c_0 in terms of the ITG mode amplitude φ_0 by matching the electron and ion region solutions in the region $\bar{k} \gg 1$. We can then fully determine the amplitude of the magnetic perturbation at the resonant surface, $x = 0$.

To achieve this, the expression (46) must be matched to the large $\bar{k}$ limit of the ion region solution, namely equation (33), to obtain:

$$\frac{\delta}{\rho_\mathrm{i}}\frac{R_1}{R_0} = \frac{2}{\pi}\frac{b_+}{b_-} \tag{47}$$

After substituting equations (22) and (44) we find

$$c_0 = \mathrm{i}\frac{\bar{\omega}_n b_0^{1/2}}{\alpha\tau}\left[\frac{\delta}{\rho_\mathrm{i}}G_n(\lambda_n) - \frac{\pi}{2\tau}\left(\frac{1.71}{2}\right)^{1/2}\left(\frac{\bar{\omega}_n}{\alpha}\right)^{3/2} \times \left(\frac{L_{T_\mathrm{i}}}{L_{T_\mathrm{e}}}\right)^{1/2} b_0\hat{\beta}_\mathrm{T}F_n(\lambda_n)\right]\left[\frac{\delta}{\rho_\mathrm{i}} - \frac{\pi}{2\tau}\left(\frac{1.71}{2}\right)^{1/2} \times \left(\frac{\bar{\omega}_n}{\alpha}\right)^{3/2}\left(\frac{L_{T_\mathrm{i}}}{L_{T_\mathrm{e}}}\right)^{1/2} b_0\hat{\beta}_\mathrm{T}\right]^{-1} \hat{\beta}_\mathrm{T}b_0^2\varphi_0, \tag{48}$$

where we have ignored terms of order $\bar{\omega}_n^2\hat{\beta}_\mathrm{T}b_0^2(\ln(\delta/\rho_\mathrm{i}) + \gamma - 1)/\alpha^2(1+\tau)\tau \ll 1$, $\gamma = 0.577\,21\ldots$ being the Euler–Mascheroni constant. As noted above, the term arising from the $\Lambda/\bar{k}$ corrections to H continues smoothly from the ion to electron regions and plays no part in the matching condition.

In the stability theory of semi-collisional tearing modes [15], such a matching condition determines the eigenfrequency ω, whereas in the present calculation it determines the amplitude c_0, the frequency having already been determined by the earlier ITG mode analysis.

In order to determine the magnetic perturbation at $x = 0$, we require $A(0) = A_0$. This can be obtained in terms of b_+ through equation (43) with b_+ in turn determined by matching corresponding powers in equations (33) and (46). Thus

$$b_+ = -\left(\frac{\delta}{\rho_\mathrm{i}}\right)^2\left(c_0 - \mathrm{i}\frac{\bar{\omega}_n\hat{\beta}_\mathrm{T}b_0^{5/2}}{\alpha\tau}G_n(\lambda_n)\varphi_0\right) \tag{49}$$

so that

$$A_0 = -\frac{2}{\pi}\frac{\tau}{\sqrt{1.71}\hat{\beta}_\mathrm{T}}\left(\frac{L_{T_\mathrm{e}}}{L_{T_\mathrm{i}}}\right)^{1/2}\left(\frac{\alpha}{\bar{\omega}_n b_0}\right)^{3/2}\left(\frac{\delta}{\rho_\mathrm{i}}\right)^2 \times \left(c_0 - \mathrm{i}\frac{\bar{\omega}_n b_0^{1/2}}{\alpha\tau}G_n(\lambda_n)\hat{\beta}_\mathrm{T}b_0^2\varphi_0\right) \tag{50}$$

and finally

$$A(0) = \frac{\mathrm{i}}{\sqrt{2}}\frac{\bar{\omega}_n}{\alpha\tau}\left(\frac{\delta}{\rho_i}\right)^2 \times \frac{K_n(\lambda_n)}{\frac{\delta}{\rho_\mathrm{i}} - \frac{\pi}{2}\sqrt{\frac{1.71}{2}}\frac{b_0\hat{\beta}_\mathrm{T}}{\tau}\left(\frac{L_{T_\mathrm{i}}}{L_{T_\mathrm{e}}}\right)^{1/2}\left(\frac{\bar{\omega}_n}{\alpha}\right)^{3/2}} b_0^2\hat{\beta}_\mathrm{T}\varphi_0 \tag{51}$$

where

$$K_n(\lambda_n) = G_n(\lambda_n) - F_n(\lambda_n) = \frac{c_n}{\sqrt{\lambda_n}}\frac{2}{\pi}\int_0^\infty \mathrm{d}y' \tan^{-1}\left(\frac{y'}{\sqrt{2\lambda_n}}\right)\left(1 + \frac{y'^2}{2\lambda_n}\right)\exp\left(-\frac{y'^2}{2}\right)H_{2n+1}(y') \tag{52}$$

encapsulates the effects of the long wavelength electrostatic ITG mode.

8. The tearing parity magnetic perturbation

There are two interesting limits to consider: (i) $|\bar{\omega}_n|b_0\hat{\beta}_\mathrm{T}/\alpha^{3/2} \ll \delta_0/\rho_i$ and (ii) $\delta_0/\rho_\mathrm{i} \ll |\bar{\omega}_n|b_0\hat{\beta}_\mathrm{T}/\alpha^{3/2}$ where we recall $\delta_0 = |\delta(\bar{\omega} = 1)|$ with $\delta \propto \bar{\omega}^{1/2}$. In the lower $\hat{\beta}_\mathrm{T}$ case (i), we have

$$A_0 = \frac{\exp(\mathrm{i}\pi/4)}{\sqrt{2}\tau}\hat{\beta}_\mathrm{T}b_0^2\left(\frac{\delta_0}{\rho_\mathrm{i}}\right)\left(\frac{\bar{\omega}_n^{3/2}}{\alpha}\right)K_n(\lambda_n)\varphi_0, \tag{53}$$

whereas in the higher $\hat{\beta}_\mathrm{T}$ case (ii):

$$A_0 = -\frac{2b_0}{\pi\sqrt{1.71}}\left(\frac{L_{T_\mathrm{e}}}{L_{T_\mathrm{i}}}\right)^{1/2}\left(\frac{\delta_0}{\rho_\mathrm{i}}\right)^2\alpha^{1/2}\bar{\omega}_n^{1/2}K_n(\lambda_n)\varphi_0. \tag{54}$$

Now

$$\frac{\delta B_x(0)}{B} \sim k_y\frac{A_\parallel(0)}{B} \sim k_y\frac{b_0^{1/2}T_\mathrm{i}}{\omega e B L_\mathrm{s}}A(0) = \frac{b_0^{3/2}}{\alpha^{1/2}\bar{\omega}_n}A_0, \tag{55}$$

so that at lower $\hat{\beta}_\mathrm{T}$

$$\frac{\delta B_x(0)}{B} \sim \left(\frac{\delta_0}{\rho_\mathrm{i}}\right)\frac{\hat{\beta}_\mathrm{T}b_0^{7/2}\bar{\omega}_n^{1/2}}{\tau\alpha^{3/2}}K_n(\lambda_n)\frac{e\varphi_0}{T_\mathrm{i}}, \tag{56}$$

while at higher $\hat{\beta}_\mathrm{T}$

$$\frac{\delta B_x(0)}{B} \sim \left(\frac{\delta_0}{\rho_i}\right)^2\frac{b_0^{5/2}}{\bar{\omega}_n^{1/2}}\left(\frac{L_{T_\mathrm{e}}}{L_{T_\mathrm{i}}}\right)^{1/2}K_n(\lambda_n)\frac{e\varphi_0}{T_\mathrm{i}}, \tag{57}$$

where we recall $\bar{\omega}_n$ and λ_n also depend on $\alpha = (b_0^2L_\mathrm{s}/L_{T_i})^{2/3}$ and n.

We can use expressions (56) and (57) to explore the relative contributions of the higher n modes, for which $\lambda_n \gg 1$. In figure 1 we plot the real and imaginary parts of K_n as a function of n for the value of λ corresponding to $\alpha = \tau = 1$, finding that $K_n(\lambda_n) \sim$ constant for $n \gg 1$. Recalling $\bar{\omega}_n \sim (2n+1)^{1/2}$ and $\lambda_n \sim (2n+1)^{1/2}$, we deduce that, at lower $\hat{\beta}_\mathrm{T}$, $\delta B_x(0)/B \propto n^{1/4}\hat{\beta}_\mathrm{T}$, so that the linear slope with $\hat{\beta}_\mathrm{T}$ becomes steeper. At higher $\hat{\beta}_\mathrm{T}$, $\delta B_x(0)/B \propto n^{-1/4}$, so that the perturbed magnetic field is smaller. The transition between the lower and higher $\hat{\beta}_\mathrm{T}$ cases scales as $\hat{\beta}_\mathrm{T} \propto n^{-1/2}$ so that the higher $\hat{\beta}_\mathrm{T}$ result has a lower threshold in $\hat{\beta}_\mathrm{T}$, reconciling these two scalings. However, at the lower values of $\hat{\beta}_\mathrm{T}$ there is a finite value of n, which increases as $\hat{\beta}_\mathrm{T}$ decreases, where $\delta B_x(0)/B$ is a maximum.

These features are evident in the results of figure 2, where the variation of $\delta B_x(0)/B$ (normalized to $e\varphi_0/T_\mathrm{i}$) with $\hat{\beta}_\mathrm{T}$, calculated from equation (55) but using the full expression (51) for $A(0)$, is shown for a number of n values. We take representative values of the other parameters to be $\delta_0/\rho_\mathrm{i} = 0.1$, $b_0 = 0.1$, $\alpha = \tau = 1$ and $L_{T_\mathrm{i}} = L_{T_\mathrm{e}}$. Finally figure 3 presents a three-dimensional visualization of the surface of $\delta B_x(0)/B$ in the space of $\hat{\beta}_\mathrm{T}$ and n for the same set of

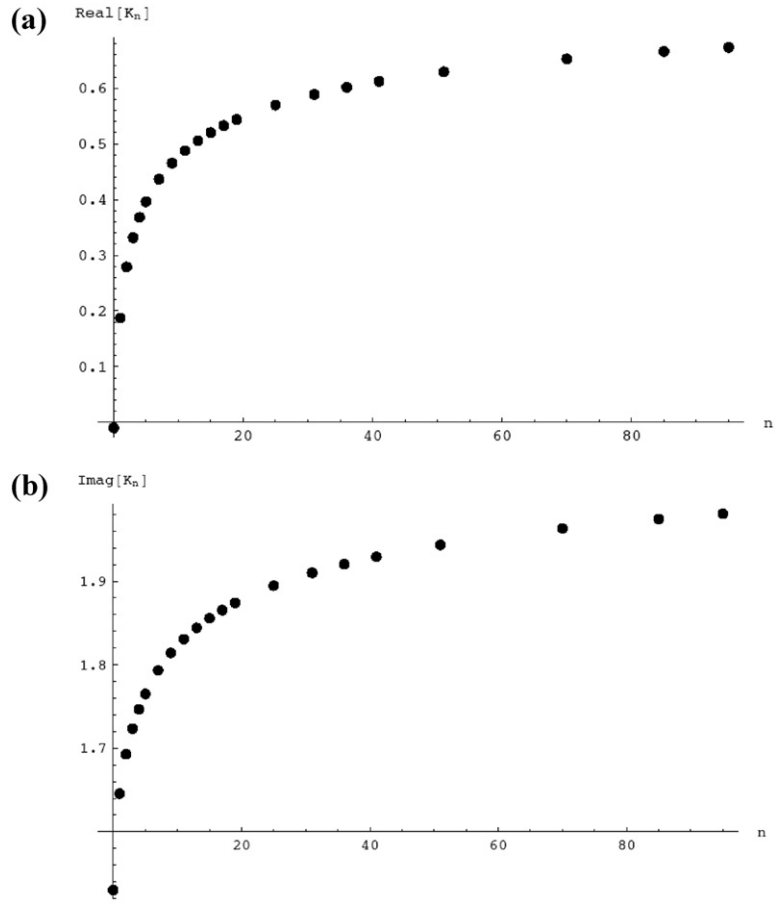

Figure 1. The integral K_n as a function of n for the case $\alpha = \tau = 1$: (a) the real part and (b) the imaginary part.

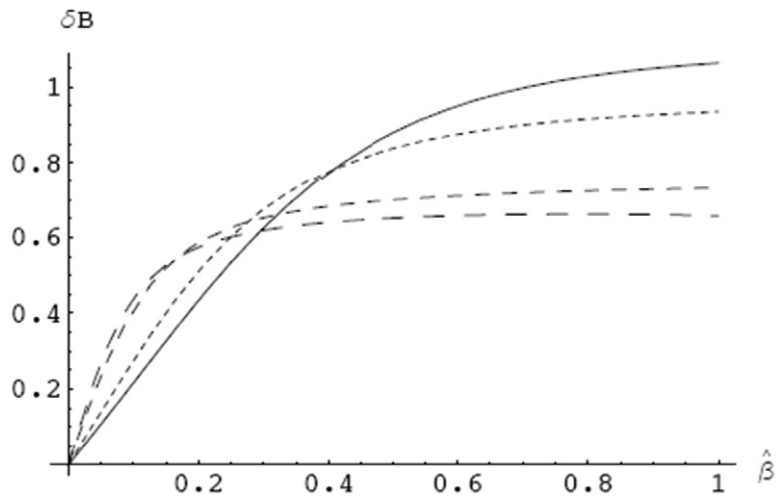

Figure 2. The variation of $\delta B_x(0)/B$, normalized to $e\varphi_0/T_\mathrm{i}$ and in units of 2×10^{-5}, with $\hat{\beta}_\mathrm{T}$ for a number of n values: $\delta_0/\rho_\mathrm{i} = 0.1$, $\alpha = \tau = 1$, $b_0 = 0.1$ and $L_{T_\mathrm{i}} = L_{T_\mathrm{e}}$. The solid line is $n = 0$ and the dashed lines correspond to $n = 1$, $n = 11$, $n = 21$, higher n being represented by longer dashes.

the parameters. It can be seen that the variation in amplitude of $\delta B_x(0)/B$ with n is not great, despite the higher n ITG modes having larger growth rates, due to competing n-dependences of various factors in equation (51). We can therefore estimate the amount of magnetic reconnection by considering just the low n modes, removing n as an important parameter. The main feature of this figure is the variation of $\delta B_x(0)/B$ with $\hat{\beta}_\mathrm{T}$: a linear increase at lower values followed by saturation above a critical value.

We will, therefore, specialize to the case $n = 0$, corresponding to the lowest odd-k_x mode. In this case we can evaluate $K_0(\lambda_0)$ as [23]

$$K_0(\lambda_0) = \frac{1}{\pi^{1/4}\sqrt{2\lambda_0}}\left[\frac{1}{\sqrt{\pi\lambda_0}} + \frac{e^{\lambda_0}}{\lambda_0}(1 - \mathrm{erf}(\sqrt{\lambda_0}))\right]. \quad (58)$$

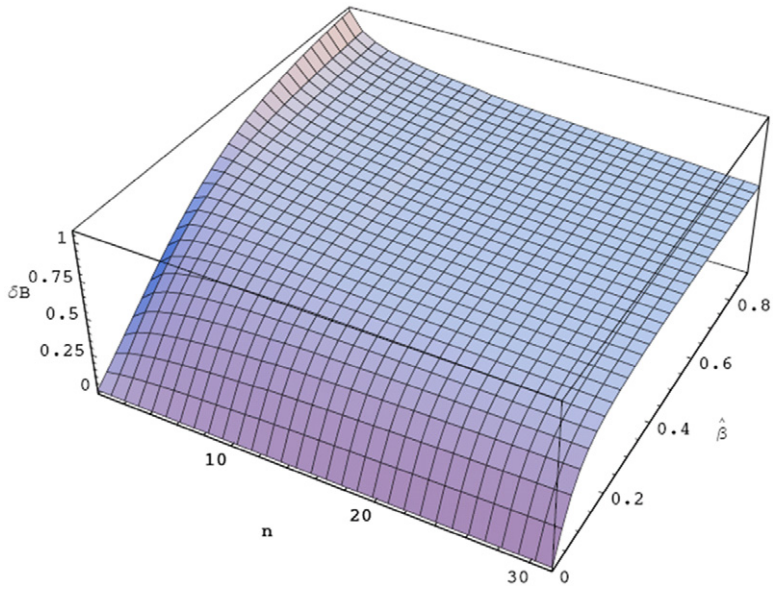

Figure 3. A three-dimensional plot showing the surface of $\delta B_x(0)/B$, normalized to $e\varphi_0/T_\mathrm{i}$ and in units of 2×10^{-5}, as a function of $\hat{\beta}_\mathrm{T}$ and n for the case: $\delta_0/\rho_\mathrm{i}=0.1$, $\alpha=\tau=1$, $b_0=0.1$ and $L_{T_\mathrm{i}}=L_{T_\mathrm{e}}$.

To express our results in more physically meaningful parameters we recall that $\delta_0/\rho_\mathrm{i}=b_0^{-5/12}(m_\mathrm{e}/2m_\mathrm{i})^{1/4}(T_\mathrm{i}/T_\mathrm{e})^{1/2}(\nu_\mathrm{ei}L_\mathrm{s}/v_\mathrm{the})^{1/2}(L_\mathrm{s}/L_{T_\mathrm{i}})^{1/6}$; it is thus useful to extract the dependences on the wavenumber b_0 and τ, writing:

$$\delta_0/\rho_\mathrm{i}=b_0^{-5/12}\tau^{-1/4}\hat{\delta},\quad \hat{\delta}=2^{-3/2}(m_\mathrm{e}/m_\mathrm{i})^{1/4}\times(\nu_\mathrm{ei}L_\mathrm{s}/v_\mathrm{the})^{1/2}(L_\mathrm{s}/L_{T_\mathrm{i}})^{1/6}. \tag{59}$$

We can consider two additional limits: (i) $\alpha\ll1$, and (ii) $\alpha\gg1$, using the results in equations (9) and (10) for $n=0$. In case (i) $\bar{\omega}_0\sim\alpha^{1/4}\tau^{1/2}$ and $\lambda_0\sim\alpha^{3/4}\tau^{1/2}$; then equation (58) implies $K_0\sim\lambda_0^{-3/2}(1-\sqrt{\lambda_0/\pi})\sim\alpha^{-9/8}\tau^{-3/4}(1-\alpha^{3/8}\tau^{1/4}/\sqrt{\pi})$ since $\lambda_0\ll1$. Thus at lower $\hat{\beta}_\mathrm{T}$ we obtain

$$\frac{\delta B_x(0)}{B}\sim\frac{b_0^{-1/4}\hat{\beta}_\mathrm{T}\hat{\delta}}{\tau^{7/4}}\left(\frac{L_{T_\mathrm{i}}}{L_\mathrm{s}}\right)^{5/3}\frac{e\varphi_0}{T_\mathrm{i}}, \tag{60}$$

while for higher $\hat{\beta}_\mathrm{T}$ we have

$$\frac{\delta B_x(0)}{B}\sim\frac{\hat{\delta}^2}{\tau^{3/2}}\left(\frac{L_{T_\mathrm{e}}}{L_{T_\mathrm{i}}}\right)^{1/2}\left(\frac{L_{T_\mathrm{i}}}{L_\mathrm{s}}\right)^{5/6}\frac{e\varphi_0}{T_\mathrm{i}}. \tag{61}$$

In case (ii) $\bar{\omega}_0\sim\alpha\tau$ and $K_0\sim\lambda_0^{-1}\sim\alpha^{-3/2}\tau^{-1}$ so that at lower $\hat{\beta}_\mathrm{T}$ we find

$$\frac{\delta B_x(0)}{B}\sim\frac{b_0^{-1/4}\hat{\beta}_\mathrm{T}\hat{\delta}}{\tau^{7/4}}\left(\frac{L_{T_\mathrm{i}}}{L_\mathrm{s}}\right)^{5/3}\frac{e\varphi_0}{T_\mathrm{i}}, \tag{62}$$

identical to result (60), and at higher $\hat{\beta}_\mathrm{T}$

$$\frac{\delta B_x(0)}{B}\sim\frac{\hat{\delta}^2}{b_0\tau^2}\left(\frac{L_{T_\mathrm{e}}}{L_{T_\mathrm{i}}}\right)^{1/2}\left(\frac{L_{T_\mathrm{i}}}{L_\mathrm{s}}\right)^{4/3}\frac{e\varphi_0}{T_\mathrm{i}}. \tag{63}$$

The lower $\hat{\beta}_\mathrm{T}$ results for the magnetic perturbations, equations (60) and (62), decrease weakly with increasing b_0, whereas the higher $\hat{\beta}_\mathrm{T}$ ones approach a constant (with a $b_0^{1/2}$ correction) for $\alpha<1$, i.e. at longer wavelength, and fall rapidly when $\alpha>1$. The higher $\hat{\beta}_\mathrm{T}$ result (61) and result (63) match at $b_0=(L_{T_\mathrm{i}}/\tau L_\mathrm{s})^{1/2}$, i.e. at $\alpha=1$ for $\tau=1$. This value is given by equation (61) and corresponds to the situation with the largest magnetic perturbation when regarded as a function of $\hat{\beta}_\mathrm{T}$ and b_0. A numerical calculation of the variation of $\delta B_x(0)/B$ with $\hat{\beta}_\mathrm{T}$ and b_0 for $n=0$, $\hat{\delta}=0.005$, $L_\mathrm{s}/L_{T_\mathrm{i}}=25$, $L_{T_\mathrm{i}}=L_{T_\mathrm{e}}$ and $\tau=1$, again calculated from equation (55) and using the full expression (51) for $A(0)$, is shown in figure 4. It illustrates the various features described above: (i) the variation of $\delta B_x(0)/B$ with $\hat{\beta}_\mathrm{T}$ consisting of a linear increase at lower values followed by saturation above a critical value; and (ii) the maximum values of $\delta B_x(0)/B$ appearing at low values of b_0 at higher $\hat{\beta}_\mathrm{T}$. An upper bound on $\delta B_x(0)/B$ imposed by the validity of the theory can be obtained by requiring $\delta_0/\rho_i<1$; equation (59) then implies

$$\frac{\delta B_x(0)}{B}<\frac{1}{b_0^{1/6}\tau}\left(\frac{L_{T_\mathrm{e}}}{L_{T_\mathrm{i}}}\right)^{1/2}\left(\frac{L_{T_\mathrm{i}}}{L_\mathrm{s}}\right)^{4/3}\frac{e\varphi_0}{T_\mathrm{i}}. \tag{64}$$

9. Stochastic field transport

In this section we use the values obtained for the magnetic perturbation at the resonant surface to estimate the resulting stochastic magnetic field transport and compare it with the basic $\boldsymbol{E}\times\boldsymbol{B}$ transport due to the original electrostatic ITG mode.

These are achieved by first inserting expression (61) for the largest 'radial' magnetic field perturbation, $\delta B_x/B$, into the Rechester–Rosenbluth formula [18] for the stochastic magnetic field contribution to the electron thermal diffusivity:

$$\chi_\mathrm{e}\sim v_\mathrm{the}\left(\frac{\delta B_x}{B}\right)^2 L, \tag{65}$$

where v_the is the electron thermal velocity and L is the correlation length along the magnetic field of the magnetic

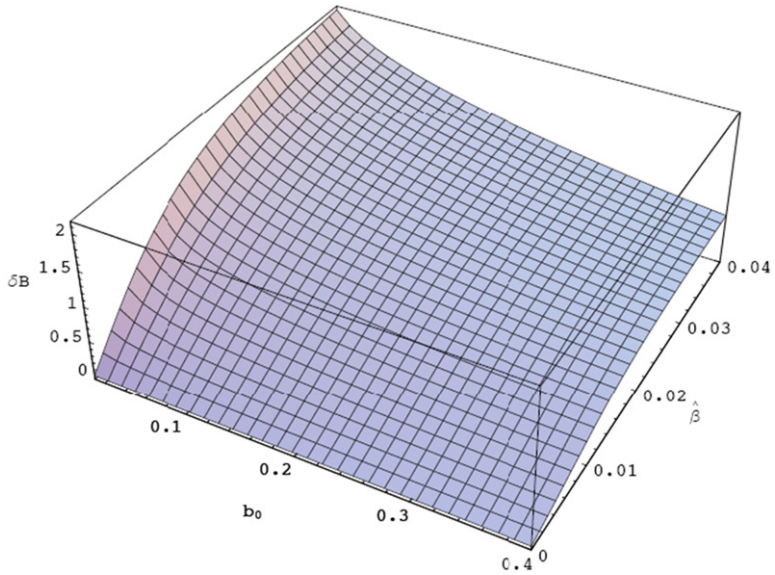

Figure 4. A three-dimensional plot showing the surface of $\delta B_x(0)/B$ normalized to $e\varphi_0/T_\mathrm{i}$ and in units of 10^{-6}, as a function of $\hat{\beta}_\mathrm{T}$ and b_0 for the case: $n = 0$, $\hat{\delta} = 0.005$, $L_\mathrm{s}/L_{T_\mathrm{i}} = 25$, $\tau = 1$ and $L_{T_\mathrm{i}} = L_{T_\mathrm{e}}$. The normalization differs from figures 2 and 3 because of the smaller value of $\hat{\delta}$.

perturbation. Taking $L \sim k_\parallel^{-1} \sim (k_y\delta_0/L_\mathrm{s})^{-1}$, we estimate the magnitude of expression (65). The result is

$$\chi_\mathrm{e} \sim \hat{\delta}^3 \frac{v_\mathrm{the} L_\mathrm{s}}{b_0^{1/12}\tau^{11/4}} \frac{L_{T_\mathrm{e}}}{L_{T_\mathrm{i}}} \left(\frac{L_{T_\mathrm{i}}}{L_\mathrm{s}}\right)^{5/3} \left(\frac{e\varphi_0}{T_\mathrm{i}}\right)^2. \tag{66}$$

It can be seen that it is a very weak function of b_0 but of course depends on φ_0, the amplitude of the ITG mode. For orientation, we can make a tentative estimate for this using a mixing-length model for the nonlinear saturation of the ITG mode:

$$\frac{e\varphi}{T_\mathrm{i}} = c\frac{1}{k_y L_{T_\mathrm{i}}}, \tag{67}$$

with c some constant, leading to the result

$$\chi_\mathrm{e}^\mathrm{st} \sim c^2 v_\mathrm{thi} R \frac{\rho_\mathrm{i}^2}{L_{T_\mathrm{i}}^2} \frac{\varepsilon^{9/4}\nu_{*_\mathrm{e}}^{3/2}}{q^{1/6}s^{4/3}b_0^{13/12}\tau^{11/4}} \left(\frac{m_\mathrm{e}}{m_\mathrm{i}}\right)^{1/4} \times \left(\frac{L_{T_\mathrm{e}}}{L_{T_\mathrm{i}}}\right)\left(\frac{L_{T_\mathrm{i}}}{R}\right)^{7/6}, \tag{68}$$

where, for facilitating comparison with tokamak transport, we have introduced the standard tokamak parameters: collisionality, $\nu_{*_\mathrm{e}} = \nu_\mathrm{ei} Rq/\varepsilon^{3/2}v_\mathrm{the}$ with $\varepsilon = r/R$, the inverse aspect ratio of a torus, q the safety factor and the magnetic shear, $s = (r/q)\mathrm{d}q/\mathrm{d}r$, since $L_\mathrm{s} = Rq/s$. Although the major radius, R, appears in this expression it is an artefact of introducing the collisionality parameter ν_{*_e} and expressing the shear-length L_s in terms of R, q and s, since the theory corresponds to the slab ITG branch. Expression (68) has a gyro-Bohm scaling, but with a significant dependence on b_0 and an unknown amplitude, c.

It is interesting to compare the island width, $w = (8(L_\mathrm{s}/k_y)\delta B_x/B)^{1/2}$ associated with the magnetic perturbation (61) with the reconnection width, δ_0. Using the mixing-length like estimate (67) and equation (61) for δB_x, we find that

$$\frac{w}{\delta_0} \sim \frac{c^{1/2}}{\tau^{1/2}} \left(\frac{L_{T_\mathrm{e}}}{L_{T_\mathrm{i}}}\right)^{1/4} \left(\frac{L_\mathrm{s}}{b_0 L_{T_\mathrm{i}}}\right)^{1/12}. \tag{69}$$

This implies that the linear theory is only valid if the factor c in the saturation level (67) for the ITG electrostatic potential satisfies the condition

$$c < \tau \frac{L_{T_\mathrm{i}}}{L_{T_\mathrm{e}}} \left(\frac{b_0 L_{T_\mathrm{i}}}{L_\mathrm{s}}\right)^{1/6}, \tag{70}$$

limiting the magnitude of the estimate (68).

However, since the more fundamental expression (66) depends on the magnitude of φ_0, it is perhaps more meaningful to compare it with an estimate of the actual $\delta\boldsymbol{E}\times\boldsymbol{B}$ (where $\delta E_y = -\mathrm{i}k_y\varphi$) cross-field transport due to the electrostatic ITG perturbation. Assuming a correlation time ω_0^{-1} with step-lengths $\delta E_y/\omega_0 B$

$$\chi_\mathrm{e}^{E\times B} \sim \left(\frac{\delta E_y}{B}\right)^2 \frac{1}{\omega_0} \sim b_0 \frac{v_\mathrm{thi}^2}{\omega_0} \left(\frac{e\varphi_0}{T_\mathrm{i}}\right)^2. \tag{71}$$

Thus the ratio of $\boldsymbol{E}\times\boldsymbol{B}$ transport to stochastic magnetic field transport becomes

$$\frac{\chi_\mathrm{e}^\mathrm{st}}{\chi_\mathrm{e}^{E\times B}} \sim \frac{\hat{\delta}^3}{(b_0^{1/3}\tau)^{11/4}} \left(\frac{m_\mathrm{i}}{m_\mathrm{e}}\right)^{1/2} \left(\frac{L_{T_\mathrm{e}}}{L_{T_\mathrm{i}}}\right)\left(\frac{L_{T_\mathrm{i}}}{L_\mathrm{s}}\right)^{4/3}, \tag{72}$$

where we have taken $\bar{\omega}_0 = 1$ and $\tau = 1$. This can be expressed in the form

$$\frac{\chi_\mathrm{e}^\mathrm{st}}{\chi_\mathrm{e}^{E\times B}} \sim \frac{\varepsilon^{9/4}\nu_{*_\mathrm{e}}^{3/2}}{s^{2/3}q^{5/6}(b_0^{1/3}\tau)^{11/4}} \left(\frac{m_\mathrm{e}}{m_\mathrm{i}}\right)^{1/4} \left(\frac{L_{T_\mathrm{e}}}{L_{T_\mathrm{i}}}\right)\left(\frac{L_{T_\mathrm{i}}}{R}\right)^{5/6}. \tag{73}$$

Estimating the ratio (73) for $b_0 = 0.1$ and typical JET parameters: $\nu_{*_e} = 3.10^{-2}$, $\varepsilon = 0.25, s = q = 2$, $\tau = 1, L_{T_i}/R = 0.25, m_e/m_i = 1/60$, we find a value $\chi_e^{st}/\chi_e^{E\times B} \sim 7.8 \times 10^{-5}$. The result clearly increases as b_0 decreases, but we require $b_0 > \hat{\delta}^{12/5}$ in order to ensure that the validity condition $\delta_0/\rho_i < 1$ is satisfied. This provides an upper bound for the consistency of the theory, although not necessarily a physical limit:

$$\frac{\chi_e^{st}}{\chi_e^{E\times B}} < \frac{\varepsilon^{3/5} s^{4/5} \nu_{*_e}^{2/5}}{q^{6/5}\tau^{11/4}} \left(\frac{m_i}{m_e}\right)^{3/10} \left(\frac{L_{T_e}}{L_{T_i}}\right) \left(\frac{L_{T_i}}{R}\right)^{6/5}. \quad (74)$$

Using the same JET parameters as above this yields $\chi_e^{st}/\chi_e^{E\times B} \sim 4\times 10^{-3}$. We note that consideration of the higher n modes leads to the result $\chi_e^{st}/\chi_e^{E\times B} \sim n^{-1/4}$, confirming the importance of lower n values.

10. Conclusions

To explore the possibility that the electromagnetic corrections to an essentially electrostatic instability occurring at small, but finite β can produce significant stochastic magnetic field transport, we have examined the case of the odd-parity, long wavelength ITG modes in sheared plasma slab geometry, with semi-collisional electron physics to permit reconnection.

The calculation resembles that of the finite ion Larmor radius effect on tearing mode instability [15] where the Δ' instability drive acts as a boundary condition at long radial wavelengths. In this case, using such a boundary condition one calculates the ion response in the shorter wavelength region where finite ion Larmor radius effects are important. Finally, the solution in this region is matched to that in the short wavelength region where electron dissipative effects dominate and permit magnetic reconnection to occur. This matching condition provides a dispersion relation for the tearing mode.

In the present case, however, the electrostatic ITG dynamics is found to provide a modified long wavelength boundary condition valid for $k_y\rho_i \ll k_x\rho_i \ll 1$. This involves a quantity Δ^*, characteristic of the ITG mode. The boundary condition is applied to the electromagnetic response in the ion region, $k_x\rho_i \sim 1$. This solution is then matched to the semi-collisional electron solution in the region $k_x\rho_i \sim \rho_i/\delta_0 \gg 1$. The matching provides an eigenvalue condition that determines the relative amplitude of the electromagnetic perturbation in the ion region driven by the electrostatic ITG mode. Although the higher n 'radial harmonics' of the ITG mode have greater growth rates, we find the lower values of n are more relevant for estimating the amount of reconnection. An important message from this calculation, with implications for numerical simulations, is the need to fully resolve the disparate electron and ion spatial scales in order to determine the perturbed magnetic field at the resonant surface, since subtle calculations are involved in arriving at an equation such as equation (51).

However, since the ITG frequency differs from that of a tearing mode, the perturbed magnetic field it actually drives near the resonant surface, where reconnection takes place, is greatly diminished. Introducing a mixing-length like estimate for the saturated amplitude of the ITG mode leads to a gyro-Bohm scaling for χ_e^{st}, though with a significant scaling with $b_0 = k_y^2\rho_i^2/2$: $\chi_e^{st} \sim b_0^{-12/11}$. It should be noted that our calculation has assumed that the electron layer is governed by linear physics, i.e. that the magnetic island associated with the magnetic perturbation is less than the semi-collisional width. For this to be valid we find the saturation level of the electrostatic ITG mode must be less than the mixing-length estimate, leading to a rather low value for χ_e^{st}. A direct comparison of the Rechester–Rosenbluth estimate for the resulting stochastic magnetic field transport with the $\boldsymbol{E}\times\boldsymbol{B}$ transport associated with the electrostatic ITG mode, indicates that their ratio is given by $\chi_e^{st}/\chi_e^{E\times B} \sim \varepsilon^{9/4} s^{-7/24} q^{-29/24} \nu_{*_e}^{3/2} (m_e/m_i)^{1/4} (L_{T_i}/R)^{29/24}$, in standard tokamak parameters, i.e., somewhat small. These findings, though for the slab ITG branch, are broadly in line with results from nonlinear simulations of electromagnetic toroidal ITG turbulence [16, 17] which found that the stochastic magnetic field transport directly due to the tearing parity ITG modes themselves is small. Rather, in [17] it was found that nonlinearly excited, linearly stable, micro-tearing modes, not tearing parity ITG modes, were responsible for the stochastic magnetic field transport observed in the calculations.

One can also envisage a similar calculation for other long wavelength modes such as the electrostatic trapped electron mode. This would produce an expression for Δ^* (the quantity encapsulating the influence of the electrostatic mode in driving reconnection, defined in equation (22)) that is characteristic of that mode rather than the ITG. Indeed, modes propagating in the same electron direction as a tearing mode may excite a greater electromagnetic response than the ITG mode. However, the separation of scales central to the present calculation for the long wavelength ITG mode and which allows a distinction between the driving region of k-space where the ITG mode is excited, i.e. $k_x\rho_i \ll 1$, and the region $k_x\rho_i \sim 1$ requiring the full finite ion Larmor response, may become problematic. The nature of the calculation would then be different as one would have to treat the whole ion region as one, before matching to the electron region at $k\rho_i \gg 1$.

Acknowledgments

This work was funded by the RCUK Energy Programme [grant number EP/I501045] and the European Communities under the contract of Association between EURATOM and CCFE. To obtain further information on the data and models underlying this paper please contact PublicationsManager@ccfe.ac.uk. The views and opinions expressed herein do not necessarily reflect those of the European Commission. The authors gratefully acknowledge the contribution of Professor S C Cowley in proposing this work.

Appendix A. Ion region equations

We require the ion response to the perturbed electromagnetic fields including full ion Larmor radius (FLR) effects and ion-sound effects. As we consider the ITG mode in sheared slab geometry we adopt a co-ordinate system with x normal to the

surfaces of constant density and temperature, z along the main magnetic field, $\boldsymbol{B}_0$ and with y perpendicular to both of these. The y-component of the magnetic field varies linearly with x: $B_y = xB_0/L_s$, providing the magnetic shear with scale-length L_s. Perturbations have the form $\varphi \sim \varphi(x)\exp(\mathrm{i}k_y y + \mathrm{i}k_z z - \mathrm{i}\omega t)$, where we measure x from the position where $k_\parallel(x) = 0$, i.e. $x_0 = -(k_z/k_y)L_s$. It is convenient to employ a Fourier representation to describe ion FLR effects so that $k_\parallel = k_y x/L_s \to -\mathrm{i}(k_y/L_s)\mathrm{d}/\mathrm{d}k_x$ and the ion gyro-kinetic equation can be written

$$-\mathrm{i}\omega h_\mathrm{i} + \frac{k_y}{L_s}v_\parallel\frac{\mathrm{d}}{\mathrm{d}k_x}h_\mathrm{i} = -\mathrm{i}\frac{Ze}{T_j}F_{0\mathrm{i}}(\omega - \omega_{*\mathrm{i}}^T)J_0(z_\mathrm{i})(\varphi - v_\parallel \mathrm{A}_\parallel), \tag{A.1}$$

where the perturbed ion distribution function has been expressed as

$$\delta f_\mathrm{i} = -\frac{Ze\varphi}{T_\mathrm{i}}F_{0\mathrm{i}} + h_\mathrm{i}\mathrm{e}^{\mathrm{i}L_\mathrm{i}}, \tag{A.2}$$

with

$$L_\mathrm{i} = |\boldsymbol{k}\times\boldsymbol{v}_\perp/\omega_\mathrm{ci}|\,, \qquad z_\mathrm{i} = \frac{k_\perp v_\perp}{\omega_\mathrm{ci}}, \qquad \omega_\mathrm{ci} = \frac{ZeB}{m_\mathrm{i}},$$
$$\omega_{*\mathrm{i}}^T = \omega_{*\mathrm{i}}\left[1+\eta_\mathrm{i}\left(u^2 - \frac{3}{2}\right)\right], \qquad u^2 = \frac{m_\mathrm{i}v^2}{2T_\mathrm{i}},$$
$$\omega_{*\mathrm{i}} = -\frac{k_y T_\mathrm{i}}{Ze}\frac{\mathrm{d}\ln n_\mathrm{i}}{\mathrm{d}r}, \qquad \eta_\mathrm{i} = \frac{d(\ln T_\mathrm{i})}{d(\ln n_\mathrm{i})} \equiv \frac{L_n}{L_{T_\mathrm{i}}}. \tag{A.3}$$

Here $v_\parallel$ is the particle velocity along the magnetic field, J_0 is the zero order Bessel Functions, $F_{0\mathrm{i}}$ is the Maxwellian distribution function, φ is the perturbed electrostatic potential and $A_\parallel$ is the parallel component of the perturbed vector potential.

We solve equation (A.1) by utilizing an ordering scheme appropriate to the slab ITG mode where in general we consider $\eta_\mathrm{i} \gg 1$ to justify the ion-sound expansion and ignoring ion Landau damping, introducing a small parameter, $\varepsilon = (L_{T_\mathrm{i}}/L_s)^{1/3}$, such that $\omega/\omega_{*\mathrm{i}} \sim \varepsilon^2$ and $k_\parallel v_\mathrm{thi}/\omega \sim \varepsilon$. The solution is linear in φ and $A_\parallel$ so the response to these two fields can be calculated independently. The lowest order response of h_i to φ contributes to the perturbed ion density, whereas the lowest order response to $A_\parallel$ produces a perturbed ion current. We therefore choose to define

$$h_\mathrm{i}^{(0)} = -\frac{\omega_{*\mathrm{i}}^T}{\omega}\frac{ZeF_{0\mathrm{i}}}{T_\mathrm{i}}J_0(z_\mathrm{i})\varphi, \tag{A.4}$$

while in first order we take

$$h_\mathrm{i}^{(1)} = -\mathrm{i}v_\parallel\frac{\omega_{*\mathrm{i}}^T}{\omega^2}\frac{ZeF_{0\mathrm{i}}}{T_\mathrm{i}}\left[-\frac{k_y}{L_s}\frac{\mathrm{d}}{\mathrm{d}k_x}(J_0(z_\mathrm{i})\varphi) + \mathrm{i}\omega J_0(z_\mathrm{i})A_\parallel\right], \tag{A.5}$$

so we see that our ordering scheme corresponds to comparable contributions of φ and $A_\parallel$ to $E_\parallel$. Finally, in second order, we obtain

$$h_\mathrm{i}^{(2)} = \frac{ZeF_{0\mathrm{i}}}{T_\mathrm{i}}J_0(z_\mathrm{i})\varphi - v_\parallel^2\frac{\omega_{*\mathrm{i}}^T}{\omega^3}\frac{ZeF_{0\mathrm{i}}}{T_\mathrm{i}}$$
$$\times\left[-\frac{k_y^2}{L_s^2}\frac{\mathrm{d}^2}{\mathrm{d}k_x^2}(J_0(z_\mathrm{i})\varphi) + \mathrm{i}\frac{k_y}{L_s}\omega\frac{\mathrm{d}}{\mathrm{d}k_x}(J_0(z_\mathrm{i})A_\parallel)\right] \tag{A.6}$$

yielding an electromagnetic contribution to the perturbed ion density.

Thus, the total perturbed ion density is given by the sum of the Boltzmann and non-adiabatic responses:

$$\frac{\delta n_\mathrm{i}}{n_\mathrm{i}} = -\frac{Ze\varphi}{T_\mathrm{i}} + \frac{1}{n_\mathrm{i}}\int \mathrm{d}^3v J_0(z_\mathrm{i})(h_\mathrm{i}^{(0)} + h_\mathrm{i}^{(2)}), \tag{A.7}$$

for use in the quasi-neutrality condition which equates the perturbed ion and electron densities. In appendix B we compute the perturbed electron density, which introduces the perturbed parallel electron velocity, $u_{\parallel\mathrm{e}}$. It is more convenient to express this in terms of the perturbed parallel current $j_\parallel$, which we relate to $A_\parallel$ using Ampère's law, and the perturbed ion velocity, $u_{\parallel\mathrm{i}}$, which is obtained from $h_\mathrm{i}^{(1)}$:

$$u_{\parallel\mathrm{i}} = \frac{1}{n_\mathrm{i}}\int \mathrm{d}^3v v_\parallel J_0(z_\mathrm{i})h_\mathrm{i}^{(1)}. \tag{A.8}$$

Thus

$$u_{\parallel\mathrm{e}} = u_{\parallel\mathrm{i}} - \frac{j_\parallel}{n_\mathrm{e}e} = u_{\parallel\mathrm{i}} - \frac{k_\perp^2}{\mu_0 n_\mathrm{e}e}A_\parallel. \tag{A.9}$$

Performing the integrations in equations (A.7) and (A.8), we find

$$\frac{\delta n_\mathrm{i}}{n_\mathrm{i}} = \frac{Ze\varphi}{T_\mathrm{i}}\left[\left(1-\frac{\omega_{*\mathrm{i}}}{\omega}\right)\Gamma_0 + \eta_\mathrm{i}\frac{\omega_{*\mathrm{i}}}{\omega}\frac{T_\mathrm{i}k_\perp^2}{m_\mathrm{i}\omega_\mathrm{ci}^2}(\Gamma_0-\Gamma_1) - 1\right]$$
$$+\frac{\omega_{*\mathrm{i}}}{\omega^3}\frac{k_y}{L_s}\frac{T_\mathrm{i}}{m_\mathrm{i}}\frac{Ze}{T_\mathrm{i}}\left\{\frac{k_y}{L_s}\left[\alpha_1\frac{\mathrm{d}^2\varphi}{\mathrm{d}k_x^2} + \frac{\mathrm{d}\varphi}{\mathrm{d}k_x}\frac{\mathrm{d}\alpha_1}{\mathrm{d}k_x} - \frac{\varphi}{k_\perp^2}\right.\right.$$
$$\left.\left.\times\left(\frac{2T_\mathrm{i}k^2}{m_\mathrm{i}\omega_\mathrm{ci}^2}\alpha_2 + \frac{(2k_x^2-k_\perp^2)}{2k_x}\frac{\mathrm{d}\alpha_1}{\mathrm{d}k_x}\right)\right]\right\}$$
$$+\frac{\omega_{*\mathrm{i}}}{\omega^3}\frac{k_y}{L_s}\frac{T_\mathrm{i}}{m_\mathrm{i}}\frac{Ze}{T_\mathrm{i}}\left[-\mathrm{i}\omega\left(\frac{A_\parallel}{2}\frac{\mathrm{d}\alpha_1}{\mathrm{d}k_x} + \alpha_1\frac{\mathrm{d}A_\parallel}{\mathrm{d}k_x}\right)\right] \tag{A.10}$$

and

$$u_{\parallel\mathrm{i}} = -\mathrm{i}\frac{\omega_{*\mathrm{i}}}{\omega^2}\frac{T_\mathrm{i}}{m_\mathrm{i}}\frac{Ze}{T_\mathrm{i}}\left[-\frac{k_y}{L_s}\left(\frac{\varphi}{2}\frac{\mathrm{d}\alpha_1}{\mathrm{d}k_x} + \alpha_1\frac{\mathrm{d}\varphi}{\mathrm{d}k_x}\right) + \mathrm{i}\omega\alpha_1 A_\parallel\right], \tag{A.11}$$

where

$$\alpha_1 = 2\int \mathrm{d}^3v\frac{m_\mathrm{i}v_\parallel^2}{2T_\mathrm{i}}\left(1+\eta_\mathrm{i}\left(\frac{m_\mathrm{i}v^2}{2T_\mathrm{i}} - \frac{3}{2}\right)\right)$$
$$J_0^2\left(\frac{k_\perp v_\perp}{\omega_\mathrm{ci}}\right)F_{\mathrm{Mi}}\left(\frac{m_\mathrm{i}v^2}{2T_\mathrm{i}}\right)$$
$$\alpha_2 = 2\int \mathrm{d}^3v\frac{m_\mathrm{i}v_\parallel^2}{2T_\mathrm{i}}\frac{m_\mathrm{i}v_\perp^2}{2T_\mathrm{i}}\left(1+\eta_\mathrm{i}\left(\frac{m_\mathrm{i}v^2}{2T_\mathrm{i}} - \frac{3}{2}\right)\right)$$
$$J_0^2\left(\frac{k_\perp v_\perp}{\omega_\mathrm{ci}}\right)F_{\mathrm{Mi}}\left(\frac{m_\mathrm{i}v^2}{2T_\mathrm{i}}\right), \tag{A.12}$$

so that

$$\alpha_1 = (1+\eta_\mathrm{i})\Gamma_0 + \eta_\mathrm{i}b(\Gamma_1-\Gamma_0) \equiv \bar{\alpha}_1 + \eta_\mathrm{i}\hat{\alpha}_1$$
$$\alpha_2 = \frac{1}{2}[\Gamma_0 + b(\Gamma_1-\Gamma_0)] + \eta_\mathrm{i}[2(b-1)^2\Gamma_0 - b(2b-3)\Gamma_1]$$
$$\equiv \bar{\alpha}_2 + \eta_\mathrm{i}\hat{\alpha}_2, \tag{A.13}$$

with $\Gamma_n(b) = \exp(-b)I_n(b)$ and $b = k_\perp^2\rho_\mathrm{i}^2/2$.

Appendix B. Electron region equations

In the semi-collisional regime we describe the electrons by the linearized Braginskii fluid equations: a continuity equation,

$$\omega\frac{\delta n_{\rm e}}{n_{\rm e}} = k_\parallel(x)u_{\parallel{\rm e}} + \omega_{*_{\rm e}}\frac{e\varphi}{T_{\rm e}}, \tag{B.1}$$

and a parallel momentum equation

$$-{\rm i}\omega\left[1-\frac{\omega_{*_{\rm e}}}{\omega}(1+1.71\eta_{\rm e})\right]A_\parallel + {\rm i}k_\parallel(x)\varphi - 1.71ik_\parallel(x)\frac{\delta T_{\rm e}}{e} - {\rm i}k_\parallel(x)\frac{T_{\rm e}}{e}\frac{\delta n_{\rm e}}{n_{\rm e}} = m_{\rm e}\nu_{\rm ei}(u_{\parallel{\rm e}} - u_{\parallel{\rm i}}), \tag{B.2}$$

where the perturbed electron temperature, $\delta T_{\rm e}$, is given by the electron energy equation

$$\left(\frac{3}{2}\omega + {\rm i}\kappa_{\parallel{\rm e}}k_\parallel^2(x)\right)\frac{\delta T_{\rm e}}{T_{\rm e}} = 1.71k_\parallel(x)u_{\parallel{\rm e}} + {\rm i}\eta_{\rm e}\omega_{*_{\rm e}}\kappa_{\parallel{\rm e}}k_\parallel(x)A_\parallel + \frac{3}{2}\omega_{*_{\rm e}}\eta_{\rm e}\frac{e\varphi}{T_{\rm e}}, \tag{B.3}$$

with $\kappa_{\parallel{\rm e}} = 3.2T_{\rm e}/m_{\rm e}\nu_{\rm ei}$ the parallel electron thermal diffusivity.

We solve for $u_{\parallel{\rm e}}$ from equations (B.1)–(B.3):

$$u_{\parallel{\rm e}} = -\frac{e}{m_{\rm e}\nu_{\rm ei}}\frac{[\sigma_0 + 2.1\sigma_1({\rm i}k_\parallel^2T_{\rm e}/m_{\rm e}\nu_{\rm ei}\omega)]}{[1+5.1({\rm i}k_\parallel^2T_{\rm e}/m_{\rm e}\nu_{\rm ei}\omega) + 2.1({\rm i}k_\parallel^2T_{\rm e}/m_{\rm e}\nu_{\rm ei}\omega)^2]} \times [{\rm i}\omega A_\parallel - {\rm i}k_\parallel(x)\varphi] + \frac{[1+2.1({\rm i}k_\parallel^2T_{\rm e}/m_{\rm e}\nu_{\rm ei}\omega)]}{[1+5.1({\rm i}k_\parallel^2T_{\rm e}/m_{\rm e}\nu_{\rm ei}\omega) + 2.1({\rm i}k_\parallel^2T_{\rm e}/m_{\rm e}\nu_{\rm ei}\omega)^2]}u_{\parallel{\rm i}}, \tag{B.4}$$

where we have taken $Z = 1$ and

$$\sigma_0 = 1 - \frac{\omega_{*_{\rm e}}}{\omega}(1+1.71\eta_{\rm e}), \qquad \sigma_1 = \left(1-\frac{\omega_{*_{\rm e}}}{\omega}\right). \tag{B.5}$$

Equation (B.4) provides the semi-collisional Ohm's law:

$$j_\parallel = \frac{ne^2}{m_{\rm e}\nu_{\rm ei}}\frac{[\sigma_0 + d_1\sigma_1({\rm i}k_\parallel^2T_{\rm e}/m_{\rm e}\nu_{\rm ei}\omega)]}{\left[1+d_0({\rm i}k_\parallel^2T_{\rm e}/m_{\rm e}\nu_{\rm ei}\omega) + d_1({\rm i}k_\parallel^2T_{\rm e}/m_{\rm e}\nu_{\rm ei}\omega)^2\right]}E_\parallel - \frac{{\rm i}k_\parallel^2T_{\rm e}}{m_{\rm e}\nu_{\rm ei}\omega}\frac{[d_2 + d_1({\rm i}k_\parallel^2T_{\rm e}/m_{\rm e}\nu_{\rm ei}\omega)]}{\left[1+d_0({\rm i}k_\parallel^2T_{\rm e}/m_{\rm e}\nu_{\rm ei}\omega) + d_1({\rm i}k_\parallel^2T_{\rm e}/m_{\rm e}\nu_{\rm ei}\omega)^2\right]} \times neu_{\parallel{\rm i}}, \tag{B.6}$$

with $d_0 = 5.1$, $d_1 = 2.1$ and $d_2 = 2.9$ and where the parallel electric field is given by

$$E_\parallel = {\rm i}\omega A_\parallel - {\rm i}k_\parallel(x)\varphi. \tag{B.7}$$

References

[1] Connor J W and Wilson H R 1994 *Plasma Phys. Control Fusion* **36** 719
[2] Drake J F, Gladd N T, Liu C S and Chang C L 1980 *Phys. Rev. Lett.* **44** 994
[3] Applegate D J *et al* 2004 *Phys. Plasmas* **11** 5085
[4] Told D *et al* 2008 *Phys. Plasmas* **15** 102396
[5] Doerk H, Jenko F, Peuschel M J and Hatch D R 2011 *Phys. Rev. Lett.* **102** 155003
[6] Guttenfelder W *et al* 2011 *Phys. Rev. Lett.* **102** 155004
[7] Snyder P B and Hammett G W 2001 *Phys. Plasmas* **8** 744
[8] Belli E A and Candy J 2010 *Phys. Plasmas* **17** 112314
[9] Pueschel M J, Kammerer M and Jenko F 2008 *Phys. Plasmas* **15** 102310
[10] Coppi B, Rosenbluth M N and Sagdeev R Z 1967 *Phys. Fluids* **10** 582
[11] Horton W, Choi D and Tang W M 1981 *Phys. Fluids* **24** 1077
[12] Biglari H, Diamond P H and Rosenbluth M N 1989 *Phys. Plasmas* B **1** 109
[13] Romanelli F 1989 *Phys. Fluids* B **1** 1018
[14] Cowley S C, Kulsrud R M and Hahm T S 1986 *Phys. Fluids* **29** 3230
[15] Connor J W, Hastie R J and Zocco A 2012 *Plasma Phys. Control. Fusion* **54** 035003
[16] Nevins W, Wang E and Candy J 2011 *Phys. Rev. Lett.* **106** 065003
[17] Hatch D R, Pueschel M J, Jenko F, Nevins W M, Terry P W and Doerk H 2013 *Phys. Plasmas* **20** 012307
[18] Rechester A B and Rosenbluth M N 1978 *Phys. Rev. Lett.* **40** 38
[19] Miller J C P 1972 *Handbook of Mathematical Functions* ed M Abramowitz and I A Stegun (New York: Dover) chapter 19
[20] Bussac M N, Edery D, Pellat R and Soule J 1978 *Phys. Rev. Lett.* **40** 1500
[21] Coppi B, Mark J W-K and Sugiyama L 1979 *Ann. Phys.* **119** 370
[22] Pegoraro F and Schep T J 1986 *Plasma Phys. Control. Fusion* **28** 647
[23] Gradshteyn I S and Ryzhik I M 1994 *Tables of Integrals, Series and Products* (San Diego, CA: Academic)